Breast Cancer: Targets and Therapy

Dovepress
Taylor & Francis Group

Open Access Full Text Article

ORIGINAL RESEARCH

Multi-Omics Characterization of ABHD12 Across Pan-Cancer and Validation of Its Role in Promoting Proliferation and Metastasis in Breast Cancer

Jiawei Zhao[1,*], Yuting Gou[1,*], Yiyang Wang[1,*], Yongxiang Li[1], Haotian Ma[1], Yiting Xing[2], Haohao Peng[2], Chenming Guo[1,3]

[1]Department of Breast Surgery, Center of Digestive and Vascular, The First Affiliated Hospital of Xinjiang Medical University, Urumqi, People's Republic of China; [2]Department of Clinical Medicine, Xinjiang Medical University, Urumqi, People's Republic of China; [3]State Key Laboratory of Pathogenesis, Prevention and Treatment of High Incidence Diseases in Central Asia, The First Affiliated Hospital of Xinjiang Medical University, Urumqi, People's Republic of China

*These authors contributed equally to this work

Correspondence: Chenming Guo, Email gcm_xjmu@yeah.net

Purpose: ABHD12 is linked to cancer and neurodegeneration; we systematically characterized its pan-cancer role and validated its oncogenic function in breast cancer (BRCA) to guide mechanistic studies.

Methods: We integrated multi-omics data from TCGA, GTEx, and various public platforms to analyze expression, prognosis, genetic variations, methylation, immune infiltration, and drug resistance. In qRT-PCR, Western blot, functional assays (CCK-8, wound healing, colony formation), and a nude mouse xenograft model, were conducted to validate ABHD12's role in BRCA.

Results: ABHD12 was significantly upregulated at both mRNA and protein levels across multiple cancers. High expression correlated with poorer overall survival in BRCA, GBM, LGG, LIHC, and UVM. It demonstrated strong to moderate diagnostic value. ABHD12 expression was associated with copy number variations (CNVs) across 23 cancers, but not with methylation. It also correlated with immune cell infiltration (especially with macrophage), tumor mutational burden, neoantigens, microsatellite instability, and immune-related genes in certain cancers, and was potentially linked to resistance to multiple chemotherapeutics. KEGG analysis indicated that ABHD12 may play a potential role in the AMPK pathway. In BRCA, ABHD12 was higher in tumors than normal tissues. Functional studies showed ABHD12 enhanced proliferation, invasion, and migration, while silencing suppressed these traits. In vivo, ABHD12-overexpressing cells formed larger tumors, confirming its tumor-promoting role.

Conclusion: ABHD12 may act as an oncogene across multiple cancers, linked to poor prognosis, diagnostic potential, chemotherapy resistance, and immunotherapy response. Its dysregulation is driven by CNVs rather than promoter methylation. ABHD12 might modulate macrophage polarization via the AMPK signaling pathway, leading to the remodeling of the tumor immune microenvironment. In vitro and vivo studies confirm its pro-tumorigenic role in BRCA, highlighting ABHD12 as a multifunctional biomarker and a molecular nexus linking lipid metabolism, immunity, and treatment resistance—warranting further study.

Keywords: ABHD12, pan-cancer, prognosis, tumor immunity, drug resistance

Introduction

Globally, cancerous neoplasms are the second reason for death. Based on the 2022 GLOBOCAN estimates, the global count of new cancer cases exceeded 18 million, with nearly 10 million deaths attributed to cancer.[1] Given this substantial disease burden, elucidating the key molecular mechanisms driving tumorigenesis and progression has become an urgent priority for the advancement of precise approaches for diagnostics and therapeutics. Emerging evidence highlights that tumor cells undergo metabolic reprogramming, particularly in lipid metabolism, to meet the heightened demands for energy, membrane synthesis, and signal transduction required for rapid proliferation and metastasis.[2] The α/β-hydrolase

https://doi.org/10.2147/BCTT.S554836
Received: 11 February 2026
Accepted: 23 April 2026
Published: 29 April 2026

domain (ABHD) family proteins are pivotal regulators in lipid metabolic pathways, and dysregulation of ABHD members has been increasingly implicated in cancer progression.[3]

AS a member of the ABHD family, ABHD12 acts as the dominant enzyme hydrolyzing lysoPS with high substrate specificity.[4] Additionally, ABHD12 is primarily link to the neurodegenerative disorder PHARC.[5] However, accumulating evidence suggests that its functional repertoire extends well beyond the nervous system. Notably, emerging studies have begun to uncover the biological significance of ABHD12 in oncogenesis; for instance, recent reports have identified ABHD12 as a potential prognostic biomarker in LIHC[6] and LUAD.[7] Furthermore, ABHD12 has been implicated in promoting the metastatic progression of HNSC.[8] Moreover, emerging evidence suggests that ABHD12 expression is correlated with sorafenib resistance in LIHC by modulating ferroptosis.[9] In addition, ABHD12 could modulate the functional states of immune cells.[4] Given these studies, we hypothesize that ABHD12 may play a pivotal role in the biological processes of tumors, the development of chemoresistance, and the remodeling of the tumor immune microenvironment.

Although isolated findings have been reported in specific malignancies, the comprehensive multi-omics landscape and biological functions of ABHD12 across the pan-cancer spectrum remain to be systematically elucidated. Specifically, the pan-cancer expression profile, epigenetic regulatory mechanisms, association with the tumor immune microenvironment, and predictive value for therapeutic response and drug resistance of ABHD12 are currently unknown. Given the inherent high heterogeneity of cancer, a systematic pan-cancer analysis is imperative to determine whether ABHD12 acts as a universal oncogenic driver or exhibits lineage-specific functions. This approach not only facilitates the identification of conserved molecular features but also provides novel insights into its context-dependent functions across distinct tumor types. To bridge this gap, this study presents a comprehensive pan-cancer analysis of ABHD12. Beyond encompassing the expression landscape, prognostic value, and epigenetic regulation typically covered in similar studies, we further elucidate its specific associations with distinct immune infiltration patterns and drug resistance mechanisms. More importantly, our functionally validate the oncogenic role of ABHD12 in BRCA suggested by these pan-cancer analyses, this integrative approach provides a more precise theoretical foundation for therapeutic intervention.

Materials and Methods

Systematic Evaluation of ABHD12 Expression in Diverse Cancer Types

This study integrated multi-source pan-cancer data to evaluate characteristics of ABHD12 expression. Download 33 kinds of cancer RNA-seq raw data from the TCGA database (https://portal.gdc.cancer.gov), extracting TPM treated by STAR process standardization expression values. Meanwhile, We obtained the uniformly processed transcriptome data from the UCSC Xena platform (https://xenabrowser.net/)[10], which utilizes the Toil workflow for batch processing. This dataset integrates TCGA and GTEx data that have been processed using a consistent pipeline (including alignment with STAR and quantification), resulting in normalized TPM values. This dataset which covers a total of 33 types of cancer of 18,102 samples. The distribution of tumor and normal samples of each cancer types is presented in Supplementary Table S1. Furthermore, the protein expression of ABHD12 in diverse cancers were further analyzed by UALCAN database (https://ualcan.path.uab.edu/)[11].

Assessment of ABHD12's Prognosis Across Various Cancers

Utilizing transcriptome data from the TCGA multi-omics database, we explored the prognostic implications of ABHD12 expression systematically in different forms of cancer. We combined the ABHD12 gene expression data with clinical prognostic indicators such as overall survival (OS), progression free interval (PFI), and disease specific survival (DSS). Univariate Cox regression analysis was used to evaluate the prognostic significance of ABHD12 expression. To perform Cox regression analysis, the R package "survival" was utilized.

Evaluation of ABHD12 as a Marker for Diagnosis in Various Cancers

To comprehensively analyze the diagnostic potential of the ABHD12 across various cancer types, we used the pan-cancer transcriptome dataset standardized by the Toil process provided by the UCSC Xena platform. Diagnostic performance was assessed using the receiver operating characteristic (ROC) curve, and the area under the curve was employed as the

evaluation criterion: AUC≥0.9 indicates high diagnostic accuracy, and 0.7≤AUC<0.9 indicates moderate diagnostic ability. The statistical analyses were completed based on the "pROC" package.

Build and Calibrate Nomograms

P<0.1 in univariate COX regression was utilized to filter prognostic factors, and a multivariate COX regression model was constructed. Prognostic nomograms were constructed based on the expression level of ABHD12 and clinical factors (such as T stage, etc.) to predict the survival rates. The performance of the nomogram was tested by using the Concordanceindex (C-index) and the calibration curve. The "survival" R package facilitated Cox regression analysis and proportional hazards hypothesis testing, and the "rms" R package was used for constructing a nomogram.

Analysis of Genetic Variation in ABHD12

We obtained the variations in genes of ABHD12 in different cancers on cBioportal (https://www.cbioportal.org)[12]. We utilized the GSCA platform (http://bioinfo.life.hust.edu.cn/GSCA/#/)[13] to systematically analyze the CNVs of the ABHD12 gene in various cancers, and further explored the potential correlations between these variations and the expression level of the ABHD12 gene, the prognosis, and survival outcomes of patients.

Methylation Analysis

To explore the relationship between ABHD12 methylation status and its expression,we use UALCAN database compares a variety of cancer types in tumor tissues and adjacent normal tissues in ABHD12 gene methylation in the promoter region of the level. At the same time, with the aid of Sangerbox 3.0 online platform (http://vip.sangerbox.com/).[14] The potential association between the expression level of ABHD12 and the RNA methylation regulatory factors of m1A, m5C and m6A (including "write protein" writer, "erase protein" eraser and "read protein" reader) was further analyzed.

Exploring the Link Between ABHD12 Expression and the Tumor Immune Microenvironment

Using the ssGSEA algorithm, the link between ABHD12 expression and immune cell infiltration across various cancers was assessed with 24 immune cell markers.[15] According to the ESTIMATE algorithm, calculate the StromalScore, ESTIMATEScore and ImmuneScore. Simultaneously, we systematically analyzed the association between ABHD12 expression and immune cell infiltration in different cancers by leveraging the TIMER2.0 database (http://timer.cistrome.org/)[16]. To further quantify the abundance of immune or matrix cells, we integrated multiple immune deconvolution algorithms such as EPIC, MCP-counter, CIBERSORT, TIDE, and XCELL for estimation, and visualized the results through a heat map.

The link between ABHD12 and Tumor Mutational Burden (TMB), Neoantigen (NEO) and Microsatellite Instability (MSI) in pan-cancers was analyzed using the Sangerbox 3.0 online database. And calculate the Spearman correlation between ABHD12 and immunomodulatory genes.

Association of ABHD12 with Drug and ICB Treatment Response

A systematic evaluation of the link between ABHD12 mRNA expression levels and drug sensitivity was performed using the GSCA platform. This platform integrates drug sensitivity data from the Cancer Drug Sensitivity Genomics (GDSC) and the Cancer Treatment Response Portal (CTRP). Besides, we conducted a more in-depth exploration the association between ABHD12 mRNA expression levels and cytokine treatment and immune checkpoint blockade (ICB) treatment responses by leveraging the Tumor Immune Synonymous Mouse Orthologs (TISMO) database (http://tismo.cistrome.org)[17]. Significant results were defined as adjusted p<0.05 (Benjamini-Hochberg).

Integrative Analysis of ABHD12 Function in Pan-Cancer Using Enrichment and PPInetwork Approaches

The top 126 genes functionally linked to ABHD12 were extracted from the STRING database (https://cn.string-db.org/, version 11.5)[18] and GEPIA2 platform (http://gepia2.cancer-pku.cn/#index)[19], and The construction of the PPI network was

carried out using Cytoscape software.[20] GOKEGG enrichment analysis[21] was was conducted utilizing the "clusterProfiler" package in R. Differentially expressed genes between ABHD12 high- and low-expression groups were identified based on TCGA dataset, followed by Gene Set Enrichment Analysis (GSEA). Using Benjamini-Hochberg correction, we selected results with adjusted $p<0.05$. Ridge plots were used to visualize the top 10 Reactome pathways with significant enrichment.

Patient Tissue Collection

Clinical cancer tissues and adjacent normal tissues, totaling 16 pairs (Supplementary Table S2), were gathered from patients who had BRCA surgery at the First Affiliated Hospital of Xinjiang Medical University from September 2023 to June 2024 were collected. Inclusion criteria: (1) Before the surgical procedure, no patients had received chemotherapy, radiotherapy, or hormone therapy; (2) The medical records and tissue samples were complete. Exclusion criteria: (1) Patients with non-primary BRCA; (2) Patients with distant metastasis of BRCA. The Ethics Committee at the First Affiliated Hospital of Xinjiang Medical University granted approval for this study (Ethics Number: 230714–07), and all participants gave informed consent.

Immunohistochemistry

The research involved 16 pairs of BRCA tissues along with nearby tissues. After antigen retrieval with citrate buffer, standard IHC staining was performed on the sections using a specific anti-ABHD12 antibody (ab181602, 1:500, Abcam, USA). Two pathologists evaluated the staining results blindly. Scoring of each tissue sample was determined by the intensity of staining (no staining=0; weak=1; moderate=2; strong=3) multiplied by the percentage of stained cells (positive rate≤25%=1; 26–50%=2; 51–75%=3; ≥75%=4), with a score range of 0–12: 0–5 indicated low expression; 6–12 points indicated high expression.

Cell Culture and Reagents

BRCA cell lines HCC-1937, MCF-10A, MCF-7, BT474, SK-BR-3, MDA-MB-468, BT-549, and MDA-MB-231 were purchased from Procell Life Science & Technology Co., Ltd., Wuhan, China. HCC-1937 cells were cultured in HCC-1937 cell-specific medium (CM-0093, Procell, China) supplemented with RPMI-1640, 10% FBS, and 1% penicillin-streptomycin solution (dual antibiotics). MCF-10A cells were cultured in MCF-10A cell-specific medium (CM-0525, Procell, China) supplemented with DMEM/F12, 5% HS, 20 ng/mL EGF, Hydrocortisone, Insulin, 1% NEAA, and 1% penicillin-streptomycin solution (dual antibiotics). MCF-7 cells were cultured in MCF7 cell-specific medium (CM-0149, Procell, China) supplemented with MEM (containing NEAA), Insulin, 10% FBS, and 1% penicillin-streptomycin solution (dual antibiotics). BT474 cells were cultured in BT-474 cell-specific medium (CM-0040, Procell, China) supplemented with RPMI-1640, 10 μg/mL Insulin, L-Glutamine, 20% FBS, and 1% penicillin-streptomycin solution (dual antibiotics). SK-BR-3 cells were cultured in cell-specific medium (CM-0211, Procell, China) containing McCoy's 5A, 10% FBS, and 1% penicillin-streptomycin solution (dual antibiotics). MDA-MB-468 cells were maintained in cell-specific medium (CM-0290, Procell, China) supplemented with DMEM, 10% FBS, and 1% penicillin-streptomycin solution (dual antibiotics). BT-549 cells were cultured in BT-549 cell-specific medium (CM-0041, Procell, China) supplemented with RPMI-1640, 10% FBS, Insulin, and 1% penicillin-streptomycin solution (dual antibiotics). MDA-MB-231 cells were maintained in MDA-MB-231-GFP cell-specific medium (CM-0642B, Procell, China) supplemented with 10% FBS, 1% penicillin-streptomycin solution (dual antibiotics), and DMEM. All cell lines were cultured in a humidified incubator at 37°C with 5% CO2.

Plasmid Construction and Transfection

Design three ABHD12 shRNA interference sequences and clone them into the MCS of the lentiviral vector GV493 (Supplementary Table S1). Enzymatic digestion and sequencing were used to verify these sequences. The overexpression vector used a plasmid containing the full-length ABHD12 cDNA as the template, which was amplified and then inserted into the GV385 vector. A suitable promoter was chosen to initiate expression, and sequencing confirmed this. The correct shRNA or overexpression plasmids (each 2 μg) were co-transfected with the packaging plasmid into HEK-293T cells according to the instructions of the Lipofectamine 3000 kit. The transfection was performed at a confluence of

approximately 80%, and 48 hours after transfection, the supernatant was collected, ultracentrifuged, and stored in buffer to resuspend the virus precipitate and be preserved at −80 °C.

Lentiviral Infection and Grouping

When the confluence of HCC-1937 and MDA-MB-231 BRCA cells reached approximately 80%, the above-mentioned concentrated virus suspension (MOI=8) was added, and the cells were infected for 24 hours. Then, fresh complete medium was replaced and the cells were cultured for another 48 hours. The cells were separated into the ABHD12 knockdown control group (NC-KD), the ABHD12 knockdown group (KD), the ABHD12 overexpression control group (NC-OE), and the ABHD12 overexpression group (OE). The conditions of each group were observed under a fluorescence microscope 72 hours after infection.

Extraction of RNA and qRT-PCR

Trizol (Invitrogen, Shanghai, China) was used to extract total RNA, and the SYBR Green PCR kit (Takara, Kyoto, Japan) was used to conduct qRT-PCR. The target genes were amplified in a 20 μL final reaction volume containing forward and reverse primers (Supplementary Table S3). Reactions for qRT-PCR were executed on an Applied Biosystems 7500 (Foster City, California, USA), with data analysis performed using the 2^{-}^ΔΔCT method.

Extraction of Protein and WB

The extraction of proteins from clinical samples and cells was performed using RIPA lysis buffer with PMSF protease inhibitor (both from Beyotime, Shanghai, China), and protein concentrations were determined using the BCA protein assay kit (Beyotime, Shanghai, China). Protein samples were loaded onto 10% SDS-PAGE gels for total protein separation and then transferred to PVDF membranes. After blocking, the membranes were incubated overnight at 4°C with ABHD12 antibody (PA5-72593, 1:1000, Thermo Fisher Scientific, USA). Incubation of the membranes with an HRP-conjugated secondary antibody was performed at room temperature. The blots were developed using ECL chemiluminescent reagents (Biosharp, Beyotime, China), and the results were recorded using a Bio-Rad imaging system. After stripping with antibody stripping buffer (sw3022, solarbio, China), the membranes were incubated overnight with GAPDH antibody (ab181602, Abcam, USA) as a loading control. The blots were developed and recorded as described above.

Cell Counting Kit-8 Experiments

Cell proliferation was detected using the Cell Counting Kit-8 (CCK-8; Dojindo Molecular Technologies, Japan). Cells were seeded in 96-well plates and cultured for 1–5 days. At each time point, CCK-8 reagent was added to each well and incubated at 37°C for 1.5 hours. The absorbance at 450 nm was measured with a microplate reader (Tecan Infinite, Switzerland). Each experimental group consisted of 3 wells per plate (technical replicates), and the experiment was independently repeated 3 times on separate days using different cell batches. Changes in cell proliferation were depicted using line graphs.

Clone Formation Experiments

In each well of a 6-well plate, roughly 1000 cells were seeded and cultured at a consistent temperature. After clones were formed, the original medium was removed, and the cells were washed 2–3 times with PBS. Then, cells were fixed for 20 minutes by adding 1 mL of 4% paraformaldehyde. After washing, 1 mL of 0.1% crystal violet was added to stain the cells for 20 minutes. After being stained, the cells were washed with water, allowed to air dry at room temperature, and subsequently photographed for counting. Each treatment group was set up in triplicate wells in a 6-well plate.

Transwell Experiment

Cells were detected using the Transwell migration assay kit (Corning, New York, USA). 600 μL of medium containing 10% FBS was added to the lower chamber as a chemoattractant, and the cells were cultured under 5% CO_2 and 37°C for 24 hours. The total cells that invaded the lower chamber were then fixed with 4% paraformaldehyde for 30 minutes and stained with 0.1% crystal violet (both from Beyotime, Shanghai, China). Each experimental condition was plated in 3 duplicate chambers

per experiment, with migrated cells stained and counted in 3 random fields per chamber. The cells were observed and counted at a magnification of 200× under an inverted microscope (Mshot, Guangzhou, China).

Cell Wound Scratch Assay

Each treatment group was set up in triplicate wells in a 6-well plate. MDA-MB-231 cells were seeded at 800 cells per well, and HCC-1937 cells were seeded at 1,000 cells per well. Cells were grown until they filled the entire field of view when observed under a microscope. A linear scratch was created on the monolayer of cells using the tip of a sterile 200 μL pipette. To eliminate debris, the cells were rinsed with PBS and then grown in a medium without serum. The wound area was photographed by using an inverted microscope from Lecia, Germany. ImageJ software was used to quantify the wound healing rate, calculated by: (initial wound area-wound area at time X) / initial wound area × 100%.

Animal Experiments

All experiments involving animals received approval from the Animal Ethics Committee at the First Affiliated Hospital of Xinjiang Medical University (Ethics Number: A240301-194). Six-week-old NCG mice were purchased from Jiangsu Jicui Biotechnology Co., Ltd. (15 mice in total, animal quarantine certificate number: B202411140401) and randomly divided into 3 groups (n=5 mice per group). Cells from different groups were digested, counted, and resuspended in pre-cooled PBS. The cells were mixed with Matrigel (354248, Corning, United States) at a 1:1 volume ratio on ice to achieve a final concentration of 5×10^6 cells/100 μL and inoculated subcutaneously in the right axilla of nude mice. Commencing on the seventh day post-inoculation, the tumors' longitudinal (L) and transverse (W) diameters were systematically measured at three-day intervals utilizing a caliper. Subsequently, the tumor volume was computed using the formula (volume=$0.5\times L\times W^2$). The integrity of the tumor surface skin, redness, bleeding, and pus were observed. The tumors were touched to determine if they were hard and adhered to surrounding tissues. Body weight was measured, and food and water intake were recorded. The activity status was observed. The color of the paw and lip mucosa was checked. Daily, the spread of redness and purulent secretions around the tumor were observed. If the body temperature rose above 40°C and the mice showed listlessness, further examination for sepsis was required. When the average tumor volume in the control group reached approximately 1000 mm^3 or any of the pre-defined humane endpoints occurred (① subcutaneous tumor volume in nude mice≥2000 mm^3 (or diameter≥2 cm), or tumor weight reached 10–15% of the nude mouse body weight; ② tumor ulceration, bleeding, purulent infection, or tumor invasion of joints and muscles, resulting in restricted movement of the nude mouse limbs), the mice were over-anesthetized with 5% sterile sodium pentobarbital solution (11715, Sigma-Aldrich, Germany) at a dose of 150 mg/kg. The mice were fixed and disinfected with alcohol, and the syringe was inserted into the abdominal cavity at a 45° angle for 5–8 mm. After confirming no blood or intestinal fluid by aspiration, the solution was slowly injected (injection time 10 seconds), and the mice were observed for more than 5 minutes. After the operation, observe whether the limbs of the nude mice are flaccid, the corneal reflex disappears and the breathing stops. Confirm the death before conducting subsequent experimental operations. All the personnel implementing the experiments have received at least 10 practical operation trainings and passed the assessment. Then, remove the tumor, weigh it and conduct subsequent analysis.

Statistical Analysis

Data visualization was performed using the "ggplot2" package in R software (v4.2.1). Data processing and statistical analyses were conducted using GraphPad Prism 9 and SPSS 26.0. Comparisons involving multiple groups, including qPCR validation, IHC scoring, colony formation assays, Transwell migration/invasion assays, and functional validation experiments (knock-down and overexpression), were analyzed using one-way analysis of variance (ANOVA) followed by Tukey's post-hoc test to control for multiple comparisons. For paired experimental designs, specifically paired Western Blot densitometry and paired clinical tissue IHC, paired Student's t-tests were used to account for individual variability. To evaluate time-dependent changes in CCK-8 proliferation assays and in vivo animal studies, two-way repeated measures (RM) ANOVA was utilized to assess the interaction between time and treatment groups. Non-normally distributed variables were analyzed using Spearman correlation. Survival analysis was performed using the Kaplan-Meier method, and differences between groups were compared using the Log rank test. In this study, the median served as the cutoff to classify samples into high and low ABHD12 expression groups. $p<0.05$ indicates statistical significance.

Results

Analysis of ABHD12 Gene Expression

Our analysis of the TCGA pan-cancer dataset revealed a significant upregulation of ABHD12 mRNA levels in 17 distinct types of malignant tumors compared to corresponding healthy tissues, including BLCA, BRCA, COAD, HNSC, LIHC, LUAD, among others (Figures 1A and S1). To verify these findings, we conducted cross-cohort analyses using the TCGA and GTEx joint cohort. The results showed that the level of ABHD12 mRNA significantly increased in 29 types of cancer, including ACC, BLCA, BRCA, LIHC, LGG, among others (Figure 1B). The analysis results of 23 paired cancer samples from the TCGA database showed that the ABHD12 mRNA level was significantly upregulated in 15 different types of cancer, including BRCA, COAD, HNSC, LUAD, LIHC, among others (Figure 1C).

Subsequently, we employed the UALCAN online analysis platform to assess the differential expression of ABHD12 protein levels across various cancers (Figure 1D). The findings indicated a significant upregulation in the expression levels of the ABHD12 protein in COAD, HNSC, KIRC, LIHC, LUAD, LUSC, and UCEC.

The Prognostic Significance of ABHD12 Across Various Cancers

The survival data in the TCGA database were analyzed using univariate Cox regression and KM methods. OS analysis indicated that overexpression of ABHD12 was a dangerous factor for various cancers, such as BRCA, GBM, LGG, LIHC, and UVM ($p<0.05$) (Figures 2A and S2A). DSS analysis revealed that overexpression of ABHD12 was a dangerous factor for multiple cancers, including BRCA, GBM, MESO, and UVM. Conversely, in BLCA, overexpression of ABHD12 was a protective factor ($p<0.05$) (Figures 2B and S2B). PFI analysis revealed that overexpression of ABHD12 was a risk factor for ACC, BRCA, GBM, KIRC, SARC, and UVM ($p<0.05$) (Figures 2C and S2C). It is worth noting that the expression of ABHD12 in BRCA, GBM and UVM was significantly correlated with all three prognostic indicators (OS, DSS and PFI) (Figure 2D). Our research findings suggest that increased expression of ABHD12 is associated with poor prognostic outcomes across multiple cancers.

Assessment of ABHD12's Diagnostic Potential in Various Cancers

To comprehensively evaluate the diagnostic relevance of the ABHD12 gene across a spectrum of cancers, we conducted ROC analysis using a combined cohort including TCGA and GTEx samples. The research found that ABHD12 performed well in 10 types of cancer such as BRCA, DLBC, LAML, LIHC, PCPG, READ, SARC, and TGCT, THYM, and UCEC, it has relatively high auxiliary diagnostic value (AUC≥0.9) (Figure 3A). ABHD12 demonstrated moderate auxiliary diagnostic efficacy (AUC≥0.7) in another 12 types of cancer, including ACC, BLCA, CESC, COAD, LUAD, PAAD, UCS, among others (Figure 3B).

ABHD12 Independently Predicts Outcomes in Specific Cancers

We discovered that ABHD12 independently affects the survival outcomes of patients across three types of cancer. These cancers include: BRCA, LGG and UVM. Pathologic stage (Stage III & Stage IV, HR=3.566, $p=0.035$) and elevated levels of ABHD12 expression (HR=1.436, $p=0.040$) were identified as sole independent prognostic factors in BRCA (Figure 4A and Supplementary Table S4A). In LGG, the primary treatment outcome, encompassing partial response (PR) and complete response (CR), acted as the singular independent prognostic indicator (HR=5.150, $p<0.001$) and elevated ABHD12 expression (HR=1.632, $p=0.008$) also is a sole independent prognostic factor (Figure 4B and Supplementary Table S4B). For UVM (Figure 4C and Supplementary Table S4C), independent prognostic factors included Clinical T stage (T4, HR=3.180, $p=0.022$), Age (>60, HR=3.780, $p=0.005$) and elevated ABHD12 expression (HR=4.229, $p=0.006$). The prognostic line calibration graph shows a good fit between the actual observed values and the predicted values (Figure 4D–F).

Investigation of Genetic Variants in ABHD12

We undertook a detailed examination of ABHD12 gene variations in various cancers to assess their potential as molecular therapeutic targets. Our investigation revealed that among 10,953 samples, amplification accounted for the largest proportion, while only 1.5% of the samples had structural variations in the ABHD12 gene. (Figure 5A and B). X207_splice/G207S was

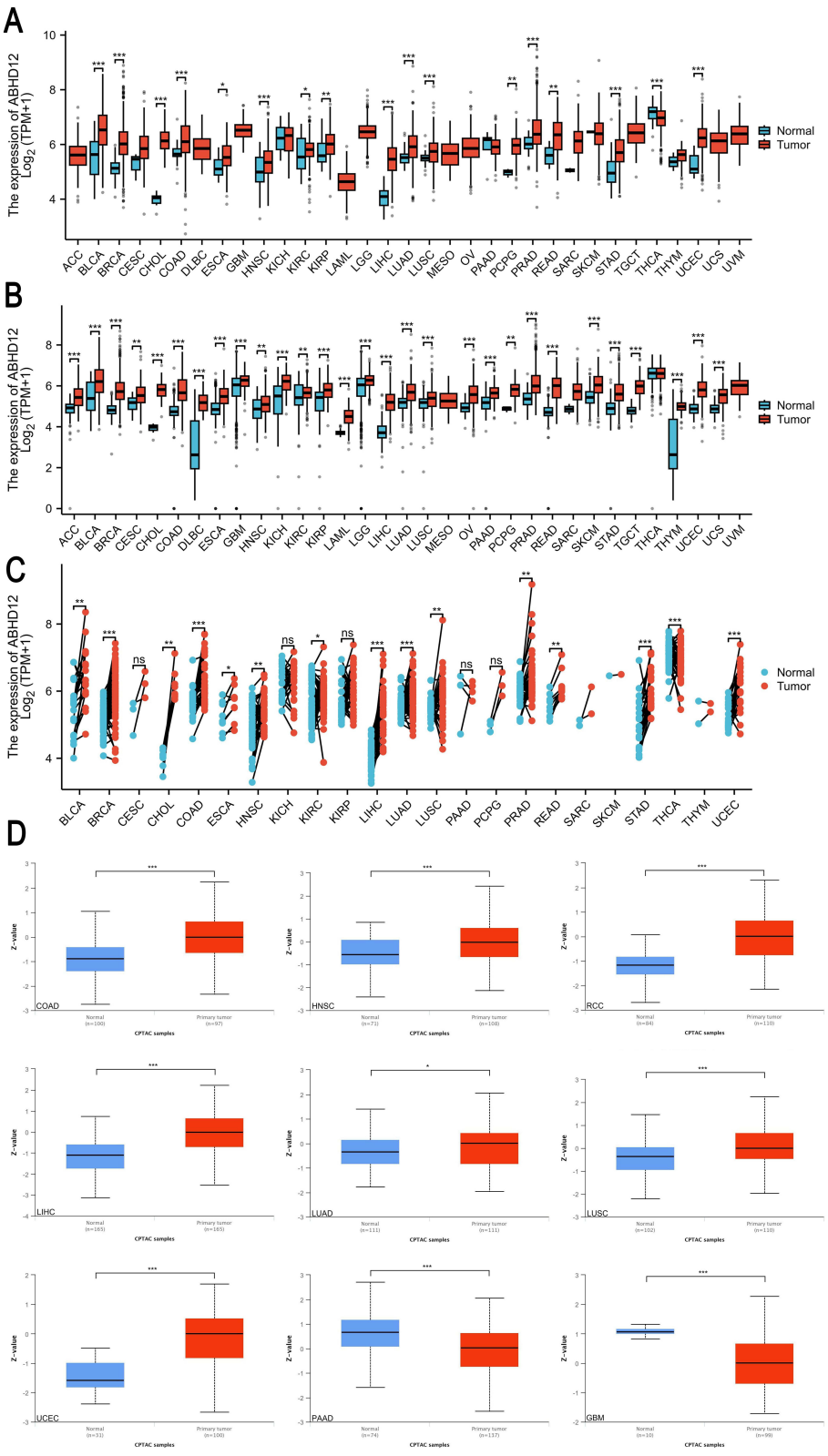

Figure 1 Differential analysis of ABHD12 mRNA expression across 33 types of cancer. Comparison of ABHD12 mRNA expression levels in tumor samples versus corresponding normal tissues based on the (**A**) TCGA dataset and (**B**) TCGA-GTEx dataset. **(C)** Comarison of ABHD12 mRNA expression between TCGA tumor samples and their paired normal tissues based on the TCGA dataset. (**D**) Expression differences of ABHD12 protein across various cancers based on the UALCAN database. **p*<0.05, ***p*<0.01, ****p*<0.001, ns represents no statistical significance.

https://doi.org/10.2147/BCTT.S554836

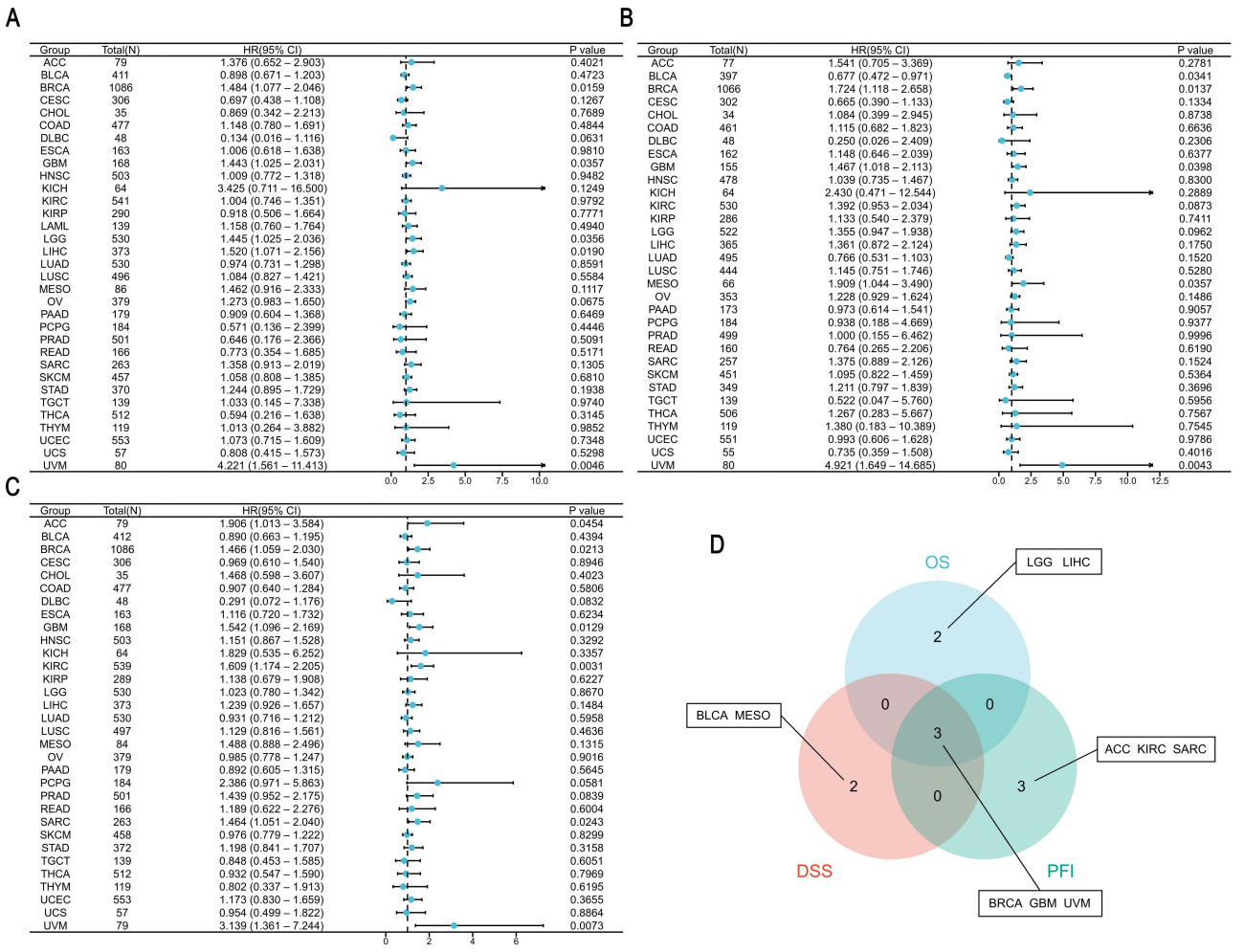

Figure 2 ABHD12 expression and its relationship with the prognosis of cancer patients. The correlation between ABHD12 expression and OS (**A**) DSS (**B**) and PFS (**C**). A Venn diagram of the analysis results of OS, DSS, and PFS in different types of cancer (**D**). Significant ($p<0.05$).

identified as a prevalent site of alteration within the ABHD12 domain (Figure 5C). The analysis based on the GSCA database shows that the ABHD12 gene exhibits CNVs in various cancers, especially in UCS, STAD, BLCA and BRCA. Among them, amplification is the main variant form (Figure S3A). Moreover, the alterations in CNVs of ABHD12 exhibit a significant positive correlation with mRNA expression across 23 types of cancer. (such as COAD, STAD, LUAD, LUSC, BRCA, READ, ESCA, HNSC, CESC, OV, ACC, LIHC, BLCA, UCEC, KIRC, SARC, PAAD, SKCM, UCS, KIRP, PRAD and GBM) (Figure S3B). Additionally, the copy number variation of the ABHD12 gene has a detrimental effect on the prognosis of patients with LGG, UCEC and UVM (Figure S3C).

ABHD12 Expression in Relation to Methylation

According to our research, ABHD12 expression correlates exclusively with the expression levels of certain members of the 24 primary m6A methylation regulators (Figure 6A). Then, the UALCAN platform was utilized to evaluate and compare the methylation levels of the ABHD12 promoter in healthy versus tumor tissues in various types of cancer. The findings indicate that the methylation levels in the promoter region of ABHD12 were significantly reduced in UCEC (p=0.038) and PRAD (p=0.0138) relative to normal tissues (Figure 6B), while they were significantly higher in COAD (p=1.61E-04), KIRC (p=8.41E-04), LUSC (p=1.62E-12), SARC (p=2.34E-02), and LIHC (p=1.27E-02) (Figure 6C).

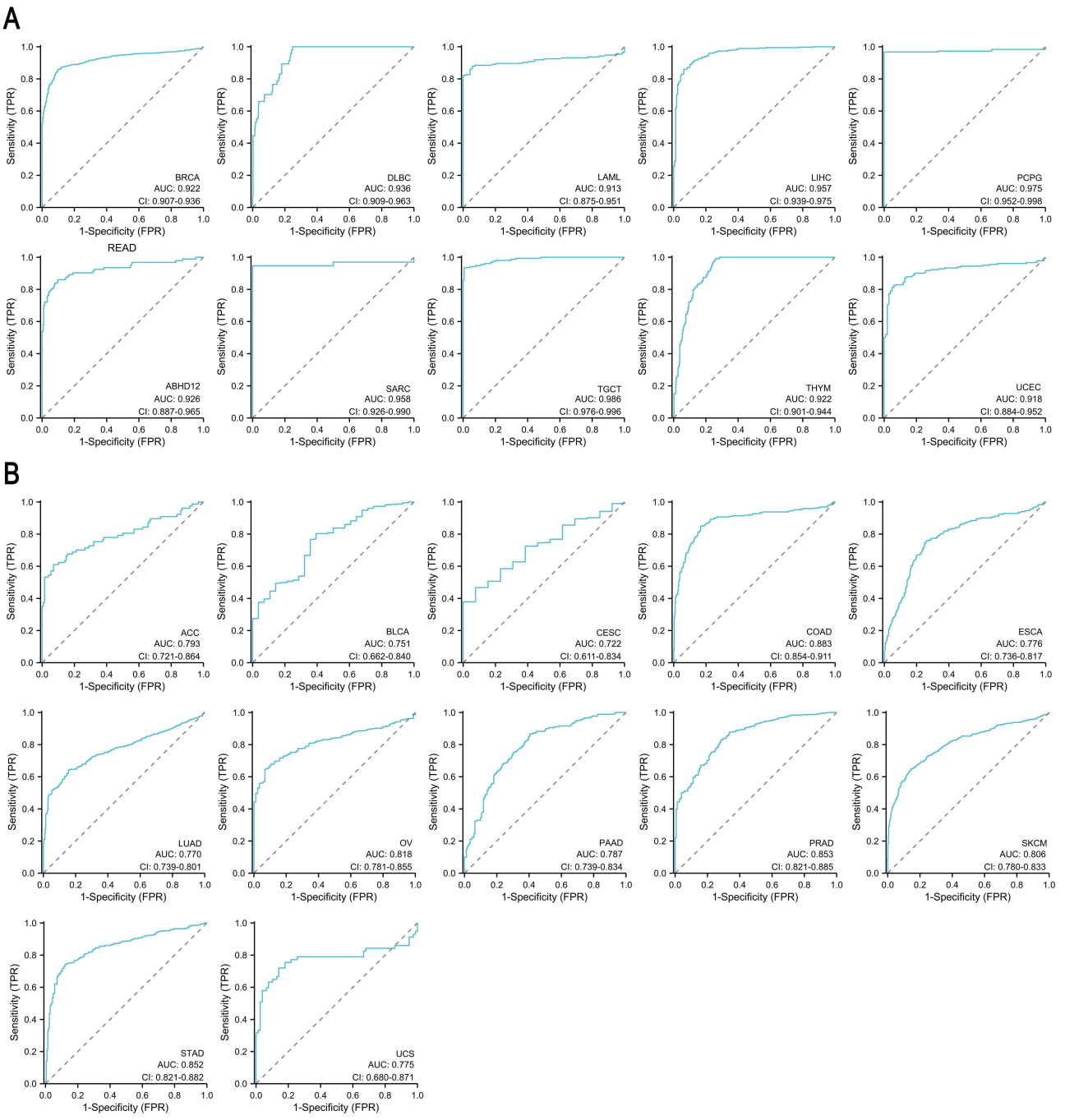

Figure 3 Analysis of the ROC for ABHD12 expression in pan-cancer. Cancer types with (**A**) high diagnostic value (AUC>0.9) and (**B**) moderate diagnostic value (AUC>0.7).

Immune Correlation Analysis of ABHD12 Expression

Our analysis revealed that in most cancers, the expression level of ABHD12 exhibited a correlation with the infiltration levels of diverse immune cell types (p<0.05) (Figures 7A and S4). Notably, in BRCA-luminal A, DLBC, HNSC, KIRC, LUAD, LUSC, MESO, SARC, TGCT, and UVM, it was linked positively to the level of phagocyte infiltration. (p<0.05) (Figure S5). Subsequently, we further investigated the correlation between the ABHD12 expression level and the StromalScore, ImmuneScore, and ESTIMATEScore in various tumors. The heatmap analysis results indicated that the expression level of ABHD12 was negatively correlated in BLCA, BRCA, COAD, LUAD, LUSC, PAAD, STAD, THCA, UCEC (p<0.05), and positively correlated in LGG and UVM (p<0.05) (Figure 7B).

https://doi.org/10.2147/BCTT.S554836

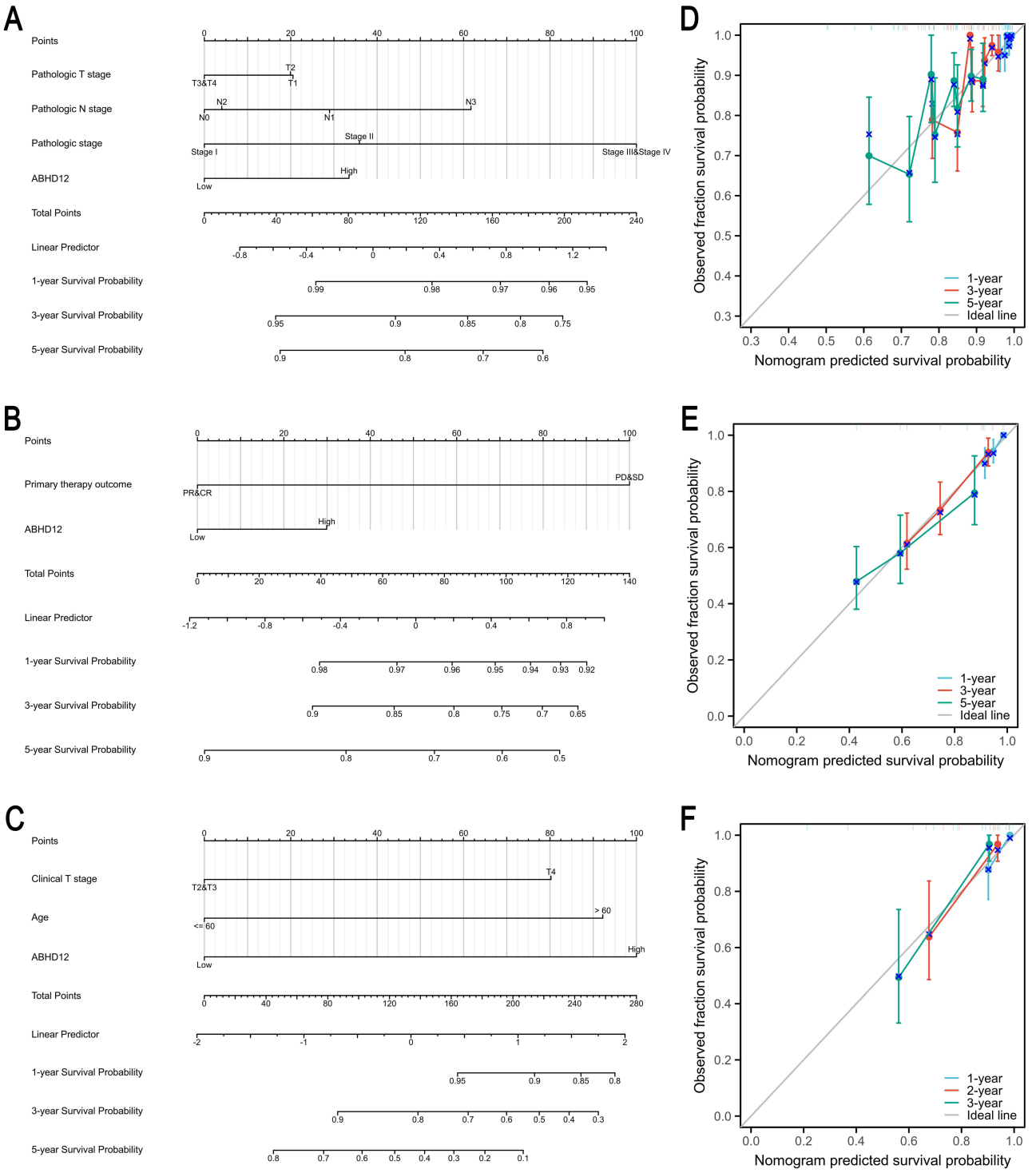

Figure 4 Prediction nomograms and calibration curves for OS of patients with four types of cancer. Nomograms for (**A**) BRCA (C-index=0.687), (**B**) LGG (C-index=0.703) and (**C**) UVM (C-index=0.792). Prognostic nomogram calibration for (**D**) BRCA, (**E**) LGG and (**F**) UVM.

The radar graph indicated a positive correlation between ABHD12 expression and TMB in SKCM, THYM, BLCA, LIHC, and LUSC, and a negative correlation in COAD, KIRC, and LGG ($p<0.05$) (Figure 7C). The MSI correlation analysis results showed a statistically significant positive relationship between ABHD12 expression levels and presence of KICH, SKCM, ESCA, KIRP, CESC, LIHC, BLCA, and LUAD ($p<0.05$), while showing a statistically significant negative correlation with COAD and TGCT ($p<0.05$) (Figure 7D). According to the NEO analysis, there is a positive

https://doi.org/10.2147/BCTT.S554836

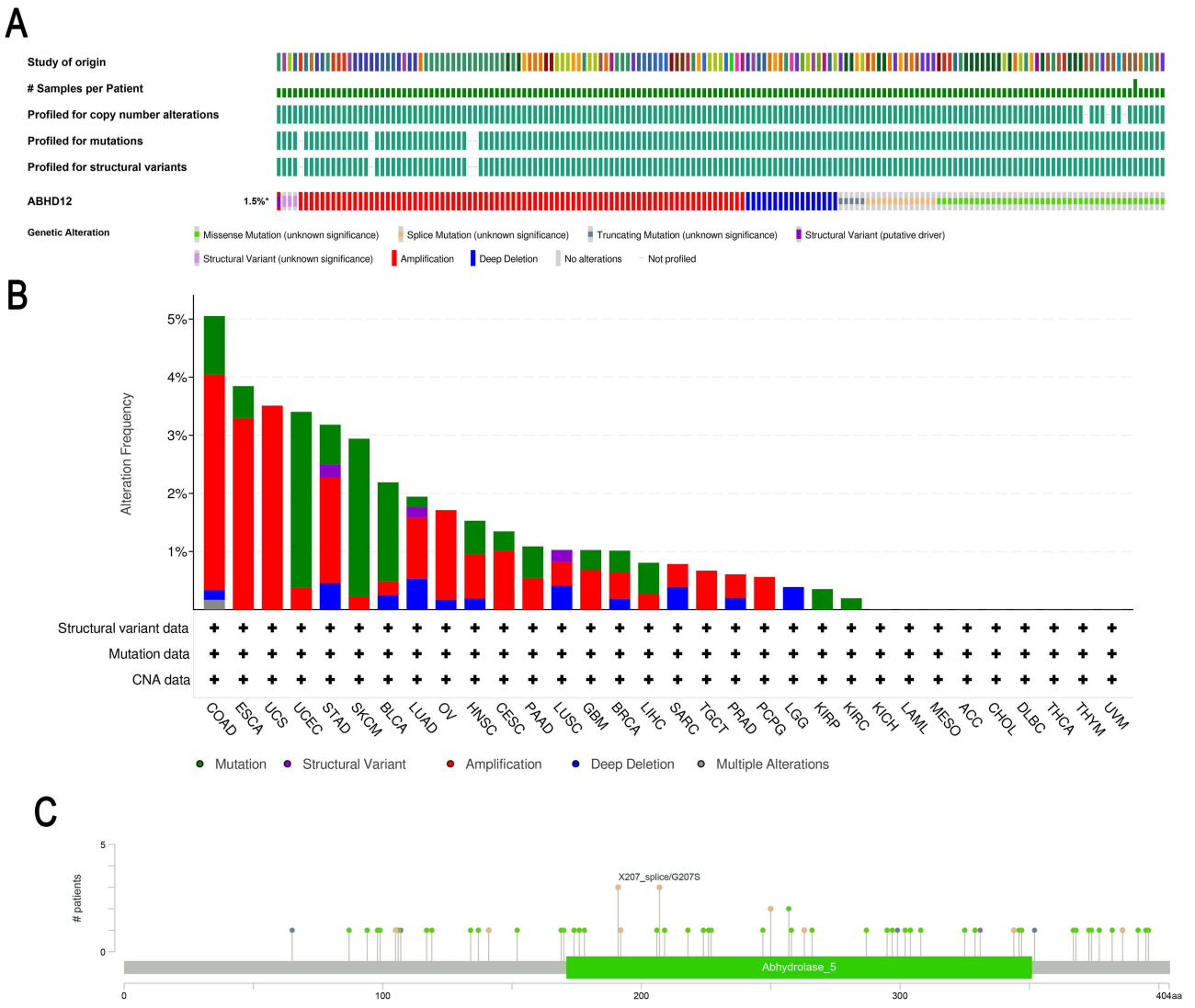

Figure 5 The mutation characteristics of ABHD12 in various tumors. (**A**) An overview of the changes in ABHD12 expression across different tumors. (**B**) Frequency distribution of different mutation types in various tumors. (**C**) Specific mutation positions marked on the ABHD12 amino acid sequence. * only 10,953 samples are profiled, # number of queried samples for each patient=1.

correlation between ABHD12 expression levels in LUAD and BRCA, but exhibited a negatively correlatedion in READ and COAD ($p<0.05$) (Figure 7E). We further analyzed the correlation between ABHD12 and the expression levels of immune function genes, and the results showed that the ABHD12 expression level was significantly correlated with various immune function genes ($p<0.05$). Among them, in BLCA, BRCA, COAD, and THCA, the expression level of ABHD12 demonstrated a negative correlation with the majority of genes associated with immune checkpoints ($p<0.05$); while in LIHC, LGG, PCPG, KIRP, HNSC, SARC, TGCT, and UVM, it was positively correlated ($p<0.05$) (Figure 7F). Furthermore, we analyzed the connection between ABHD12 expression and a curated group of immune-related genes sourced from the GSEA database, which comprises 43 markers of immune activation and 22 immunosuppressive elements. ABHD12 expression showed significant correlations with multiple genes in this set (Figure S6).

ABHD12 Correlates with Drug Sensitive and ICB Response

Firstly, Our analysis of the CTRP database revealed a positive correlation between ABHD12 mRNA expression and the IC50 values of clinically utilized drugs such as Cytarabine, Cyclophosphamide, Docetaxel, Doxorubicin, Etoposide, Gemcitabine, Mitomycin, Omacetaxine, mepesuccinate, Topotecan, and Vinblastine ($p<0.05$) (Figure 8A and Supplementary Table S5A).

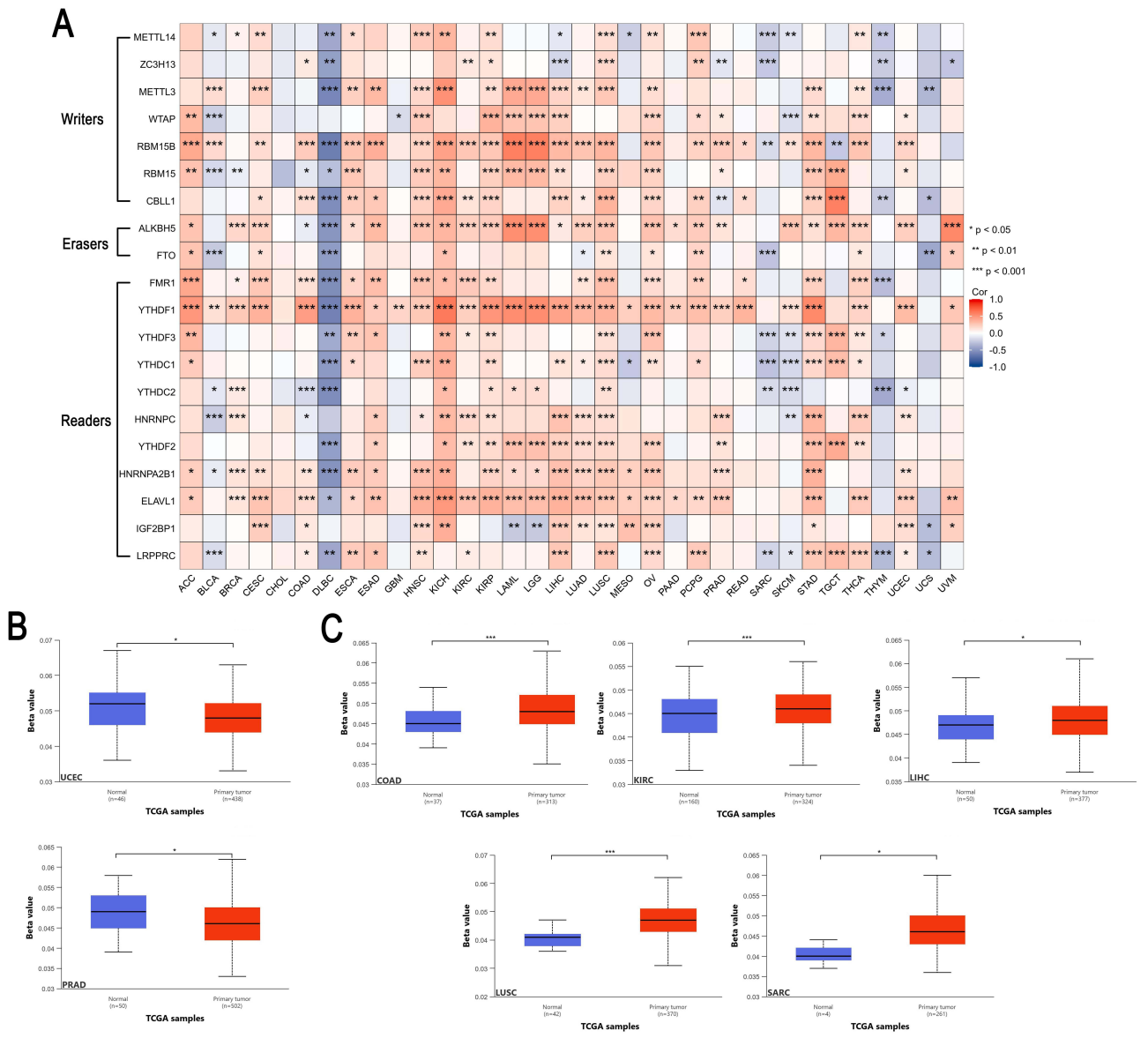

Figure 6 Epigenetic methylation analysis of ABHD12. (**A**) The association between ABHD12 mRNA expression and m6A modification-related regulatory factors in various cancers. (**B** and **C**) Analysis of the difference methylation levels of the ABHD12 promoter region between tumor and normal tissues (β values). *p<0.05, **p<0.01, ***p<0.001.

Secondly, our analysis of the GDSC database revealed that elevated ABHD12 mRNA expression, the higher the IC50 values of 5-Fluorouracil, Methotrexate, and Vorinostat (p<0.05) (Figure 8B and Supplementary Table S5B). These findings point to ABHD12 as a potential gene related to resistance to chemotherapy.

The TISMO database was used to correlate the expression levels of the ABHD12 gene in different tumor models with the responses to cytokine therapy (including IFN-β, IFN-γ, TGF-β1, TNF-α) and ICB therapy (including anti-PD-1, anti-PD-L1, anti-PD-L2, and anti-CTLA-4) in different cancer treatments. This further study and exploration aim to investigate the potential role of the ABHD12 gene in different cancers and its correlation with cytokine therapy and ICB therapy. The TISMO database includes tumor models such as BRCA (4T1, E0771, EMT6, T11, KPB25L, p53-2225 L, p53-2336R); colorectal cancer (CT26, MC38); STAD (YTN16); HNSC (MOC1, MOC22); LIHC (BNL-MEA), lung cancer (LLC); SKCM (B16, YUMM1.7, D3UV2, D4M.3A.3); pancreatic ductal adenocarcinoma (KPC, Panc02); renal adenocarcinoma (Renca); SARC (402230). Then, we compared the expression levels of the ABHD12 gene in different tumor models during cytokine therapy and ICB therapy. The results of the cytokine treatment group showed that the ABHD12 expression level in the IFN-b response group of

https://doi.org/10.2147/BCTT.S554836

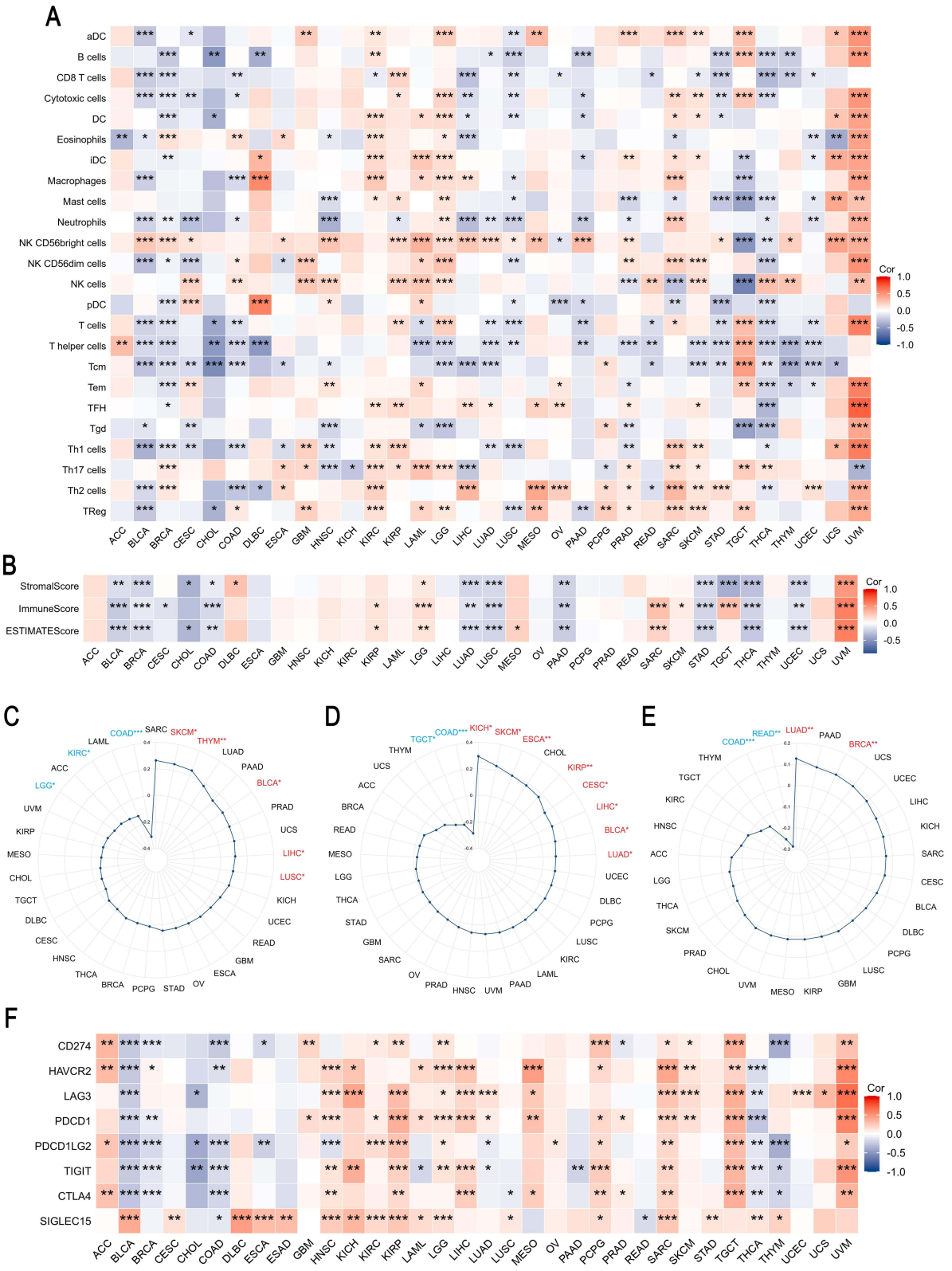

Figure 7 The relationship between immune and ABHD12 expression in pan-cancer. Analysis of the correlation between ABHD12 expression and (**A**) immune infiltration. The association of ABHD12 expression with (**B**) StromalScore, ImmuneScore, and ESTIMATEScoreABHD12 expression and its associations with (**C**) TMB, (**D**) MSI and (**E**) NEO across 33 cancer types. (**F**) The interrelationship of ABHD12 expression with immune checkpoint genes. Red text indicates positive correlations; blue text indicates negative correlations. *p<0.05, **p<0.01, ***p<0.001.

https://doi.org/10.2147/BCTT.S554836

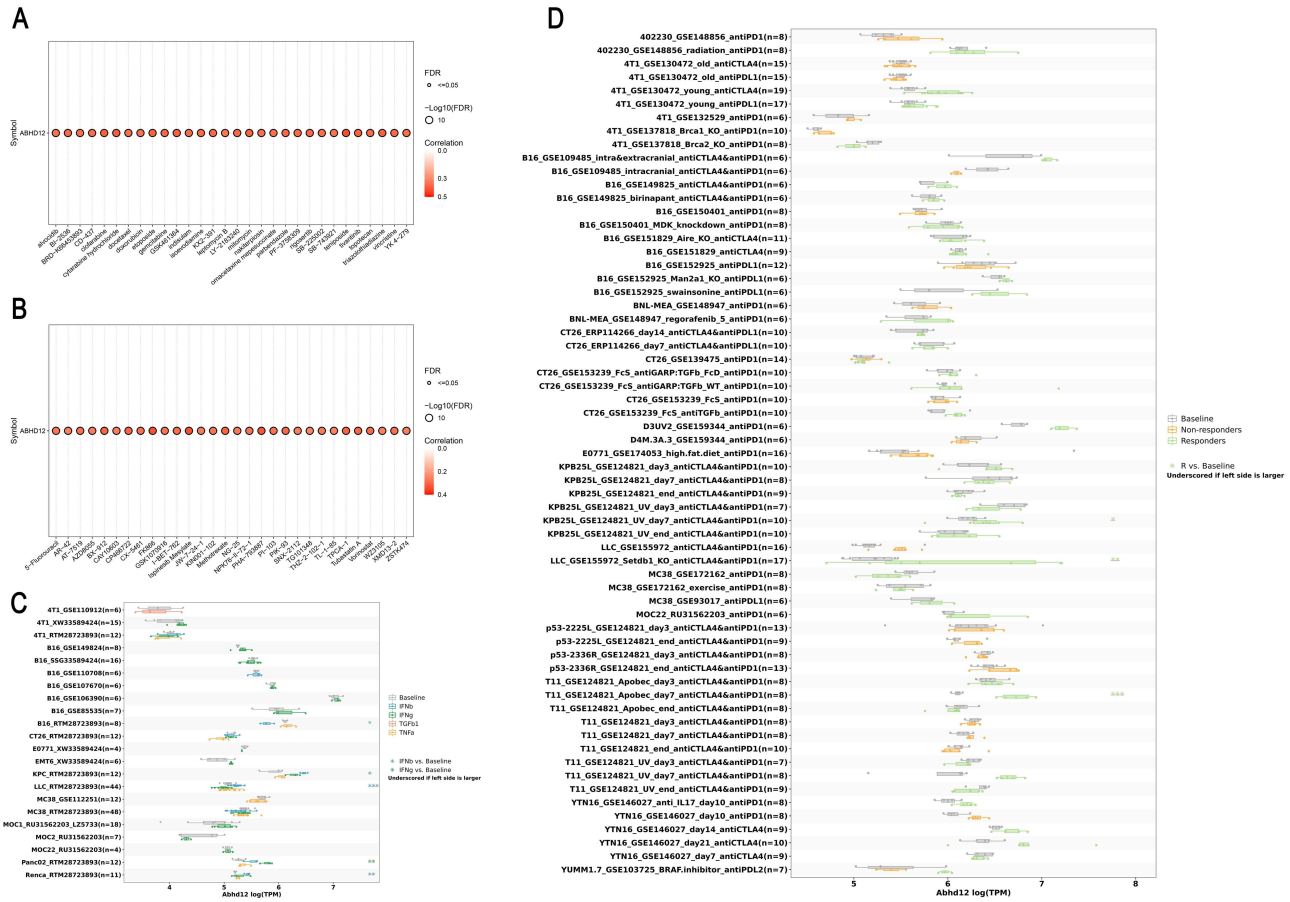

Figure 8 ABHD12 expression and drug sensitivity analysis. (**A**) Association between ABHD12 mRNA expression levels and drug sensitivity in CTRP. (**B**) Association between ABHD12 mRNA expression and drug sensitivity in the GDSC. (**C**) Correlation between ABHD12 expression levels across different tumor models and response to cytokine therapy. (**D**) Comparison of ABHD12 expression across tumor models, before versus after ICB, and between ICB responders and non-responders. *p<0.05, *p<0.05, **p<0.01, ***p<0.001.

B16_RTM28723893 (n=8) was significantly lower than the baseline (p<0.05), while the ABHD12 expression levels in the IFN-b response groups of KPC_RTM28723893 (n=12), LLC_RTM28723893 (n=44), and Renca_RTM28723893 (n=11) were significantly higher than the baseline group (p<0.05) (Figure 8C). The results of the ICB treatment group showed that the ICB treatment response groups of KPB25L_GSE124821_UV_day7_antiCTLA4andantiPD1 (n=10), LLC_GSE155972_Setdb1_KO_antiCTLA4andantiPD1 (n=17), and T11_GSE124821_Apobec_day7_antiCTLA4andantiPD1 (n=8) were significantly higher than the baseline group (Figure 8D). Hence, we consider that ABHD12 expression levels can inform the design of individualized anti-tumor treatments for patients. These findings indicate that high ABHD12 expression in certain cancers may be associated with the benefits of ICB therapy.

Uncovering the Pan-Cancer Functions of ABHD12 via Integrative Enrichment and Protein–Protein Interaction Network Approaches

In this study, the PPI network of ABHD12-related 26 genes was constructed using Cytoscape (Figure 9A) (Supplementary Table S6), and further GOKEGG analyses were conducted (Supplementary Table S7). The GO-BP analysis indicated that ABHD12 might be involved in various glycosylation modification processes (Figure 9B). In the GO-MF analysis, ABHD12 was significantly enriched in various glycosyltransferase activities (Figure 9C), further suggesting that it might play an important role in glycosylation regulation. The GO-CC analysis showed that ABHD12 was associated with lysosomal membrane, endoplasmic reticulum-Golgi transport vesicles, proton-transporting V-type ATPase complex, and autophagosome membrane (Figure 9D). The KEGG pathway analysis indicated that ABHD12 may play a role in critical biological pathways

https://doi.org/10.2147/BCTT.S554836

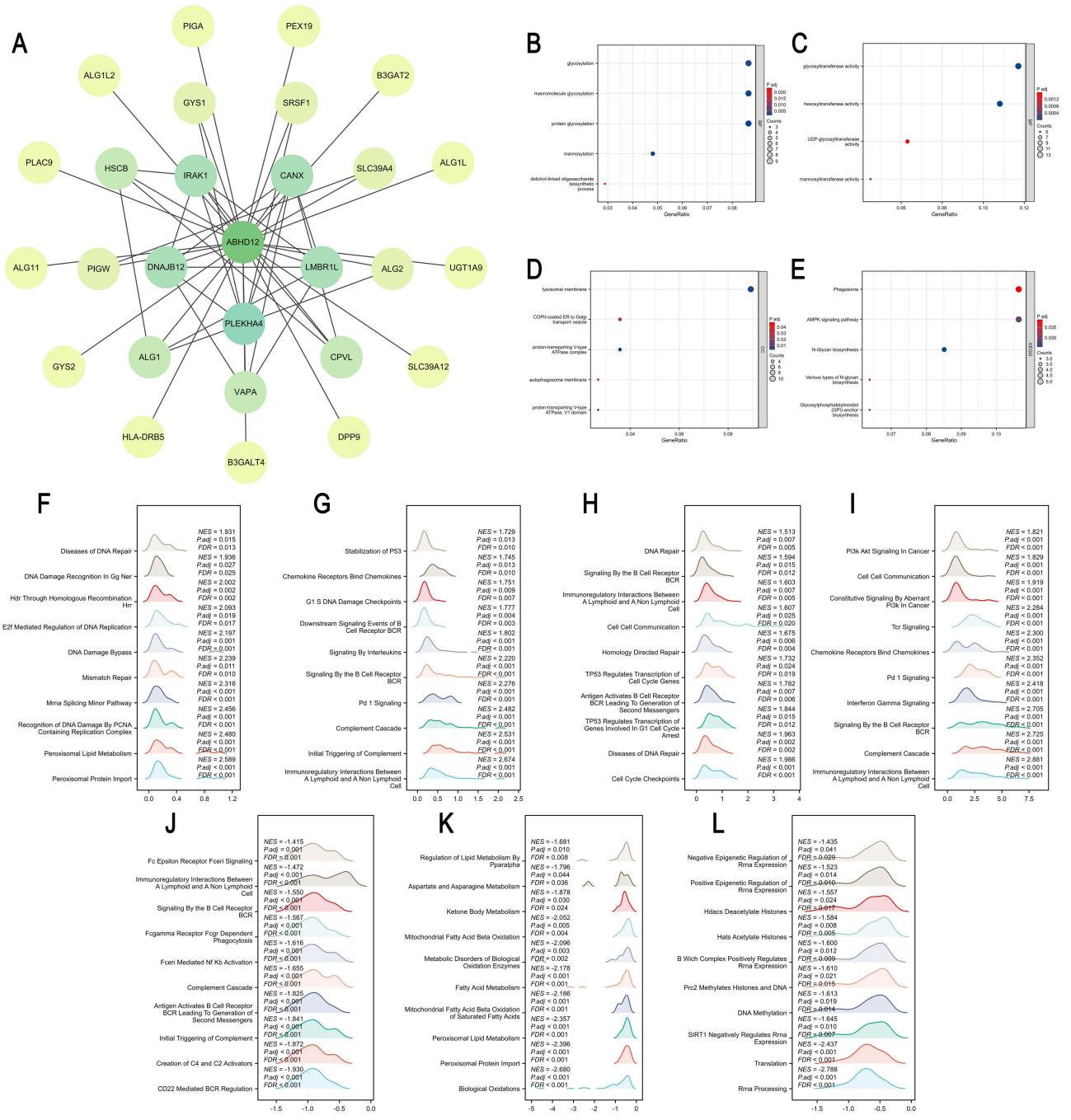

Figure 9 Analysis of the genes related to ABHD12, interaction proteins, and functional enrichment. (**A**) Protein-protein interaction (PPI) network of ABHD12. (**B**) GO biological process analysis. (**C**) GO molecular function analysis. (**D**) GO cellular component analysis. (**E**) KEGG pathway analysis. Functional enrichment analysis of ABHD12 in four types of cancer. In (**F**) BRCA, (**G**) LGG, (**H**) LIHC, (**I**) UVM, the top ten pathways are positively correlated with ABHD12 expression. In (**J**) BRCA, (**K**) LIHC, (**L**) UVM, the top ten pathways are negatively correlated with ABHD12 expression.

such as Phagosome, AMPK signaling pathway, and Glycosylphosphatidylinositol (GPI)-anchor biosynthesis (Figure 9E). These pathways are widely involved in multiple essential biological processes such as metabolic pathway, autophagy regulation, and immune response.

We conducted GSEA enrichment analysis using the Reactome pathway database. The enrichment analysis results showed that multiple key pathways were significantly enriched in BRCA, LGG, LIHC, and UVM. The enriched

 https://doi.org/10.2147/BCTT.S554836

pathways mainly involved DNA damage repair and immune regulation, suggesting that the expression level of ABHD12 may play a role in genomic stability and immune microenvironment regulation (Figure 9F–L).

Impact of ABHD12 Expression on BRCA Cell Behavior

This study detected the ABHD12 expression levels in BRCA tissues and adjacent normal tissues using Western blot and immunohistochemistry, revealing significantly elevated expression of ABHD12 in BRCA tissues compared to adjacent normal tissues (Figure 10A–D). Subsequently, qRT-PCR was employed to verify its expression in normal breast cellsand BRCA cell

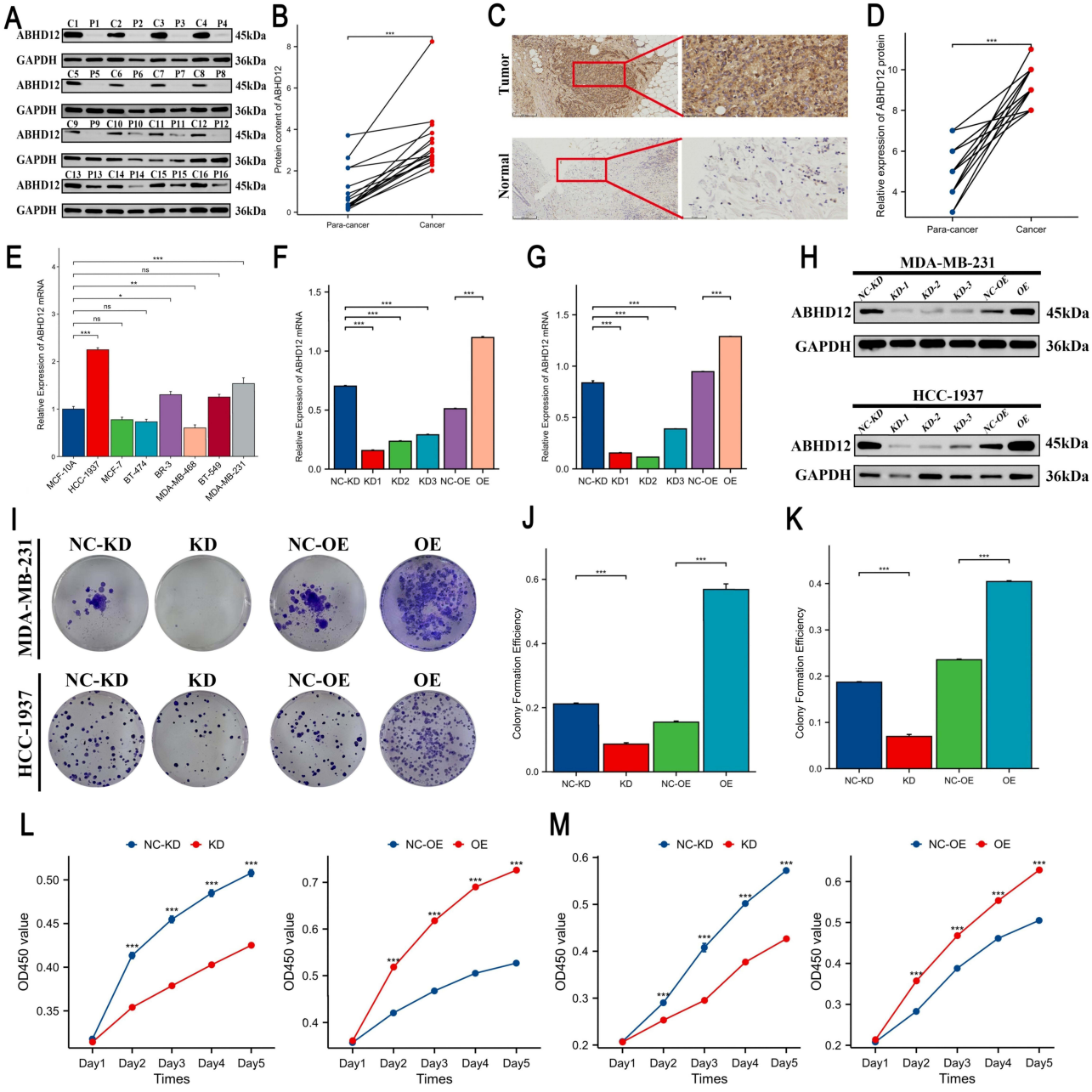

Figure 10 ABHD12 is highly expressed in breast cancer tissues and promotes the proliferative capacity of breast cancer cells. **(A** and **B)** WB experiments confirm the expression of ABHD12 protein in breast cancer tissues and adjacent normal breast tissues. **(C** and **D)** IHC experiments verify the expression and localization of ABHD12 in breast cancer tissues (cytoplasm). (**E**) RT-qPCR experiments confirm the expression of ABHD12 mRNA in normal breast cells and breast cancer cells. Verification of ABHD12 knockdown and overexpression efficiency at the mRNA level in **(F)** MDA-MB-231 cell line and (**G**) HCC-1937 cell line. (**H**) Verification of ABHD12 knockdown and overexpression protein efficiency at protein level in MDA-MB-231 and HCC-1937 cell line. (**I**) Colony formation assays and their quantitative analysis in (**J**) MDA-MB-231 and (**K**) HCC-1937 cell lines further validate the impact of ABHD12 on cell proliferation. CCK-8 experiments demonstrate the effects of different ABHD12 expression levels on the proliferative capacity of (**L**) MDA-MB-231 cell line and (**M**) HCC-1937 cell line. *p<0.05, **p<0.01, ***p<0.001; ns indicates no statistical significance.

https://doi.org/10.2147/BCTT.S554836

lines, demonstrating significant overexpression of ABHD12 mRNA in HCC-1937 and MDA-MB-231 cells (Figure 10E). Consequently, ABHD12-knockdown and overexpression cell lines were constructed for HCC-1937 and MDA-MB-231, and the efficacy of gene knockdown and overexpression was validated (Figure 10F–H). The validity of these findings was further corroborated through the use of colony formation assays (Figure 10I–K). The results of the CCK-8 assay indicate that the knockdown of ABHD12 significantly inhibits the proliferation of BRCA cells, whereas overexpression promoted proliferation (Figure 10L and M). The ability of HCC-1937 and MDA-MB-231 cells to migrate was increased by ABHD12 overexpression and decreased by ABHD12 knockdown, as shown by scratch healing assays (Figure 11A–D). Transwell experiments demonstrated that ABHD12 overexpression significantly enhanced migration and invasion, whereas ABHD12 knockdown exhibited inhibitory effects (Figure 11E–J). Furthermore, animal studies revealed that ABHD12 overexpression was associated with increased tumor volume and weight in NCG mice (Hedges' g=8.14), while ABHD12 knockdown exhibited a trend toward reducing these growth parameters (Figure 11K–N). Collectively, the results indicate that ABHD12 shows high levels of expression in BRCA and facilitates the proliferation, migration, and invasive potential of BRCA cells.

Discussion

Previous investigation on ABHD12 have been limited to a single cancer type and have not conducted a systematic exploration at the pan-cancer level regarding its genomic or epigenetic regulatory mechanisms, its correlation with the tumor immune microenvironment and its connection to critical immunotherapy biomarkers (such as TMB, MSI, and NEO), and the correlation between ABHD12 expression and anti-tumor drug sensitivity (such as chemotherapy drugs and ICB). Our approach is informed by established pan-cancer methodologies and statistical analysis methods that link genomic features to clinical relevance.[22–24] This research encompasses an extensive pan-cancer analysis involving 33 distinct cancer types, validates ABHD12 expression differences in clinical BRCA samples, and functionally demonstrates its role in promoting proliferation, migration, and invasion of BRCA cells in vitro, as well as in a mouse xenograft model. Collectively, this work provides the first systematic characterization of ABHD12's regulatory networks, immune-related features, and therapeutic predictive value across multiple cancers, thus addressing a significant gap in the existing knowledge of this gene.

The ABHD superfamily represents one of the most functionally diverse and widely distributed enzyme families identified to date. Its members encompass a broad range of enzymatic activities, including proteases, lipases, esterases, dehalogenases, peroxidases, and cyclo-oxidase hydrolases, among others.[25] Recent studies have demonstrated that ABHD8 can modulate inflammatory responses through partner protein-mediated autophagy.[26] Furthermore, dysregulation of S-palmitoylation has been firmly implicated in the pathogenesis of cancer and various immune-related disorders.[27] Within the ABHD family, several members are known to regulate S-palmitoylation dynamics. For instance, ABHD10 functions as a de-palmitoylase that modulates cellular oxidative stress responses by controlling the activity of the antioxidant protein PRDX5,[28] while ABHD16A exhibits robust de-palmitoylase activity and plays a critical role in the interferon-induced transmembrane (IFITM)-mediated antiviral immune response.[29] However, current knowledge regarding the tumor biological functions of ABHD12 remains highly limited. As a member of this superfamily, ABHD12 possesses a conserved α/β-hydrolase domain, raising the possibility that it may similarly contribute to the regulation of S-palmitoylation, autophagy, and immune signaling pathways in tumor, which warrants further investigation.

ABHD12 may represent a potential candidate factor implicated in tumorigenesis. Our analyses reveal that ABHD12 is markedly overexpressed in various cancer types relative to normal tissues and exhibits a significant correlation with adverse clinical prognosis. Survival analysis demonstrates that increased expression of ABHD12 is significantly associated with decreased overall survival in patients with BRCA, GBM, LGG, LIHC, and UVM. These findings are corroborated by a recent independent study, which similarly reported upregulation of ABHD12 in LIHC tissues and its association with adverse patient outcomes.[6,9] Furthermore, analysis of the ROC curve shows that elevated ABHD12 expression provides moderate to strong support for diagnosis in most cancer types, suggesting its potential utility as a universal diagnostic biomarker. It is important to acknowledge that this study primarily relies on bioinformatic analyses of public databases. Although batch effect correction was performed, bulk RNA-seq results may still be susceptible to inherent technical and biological biases. Furthermore, prognostic survival analysis was restricted to univariate models due to sample size constraints. Consequently, prospective validation in large-scale clinical cohorts is warranted to confirm diagnostic efficacy.

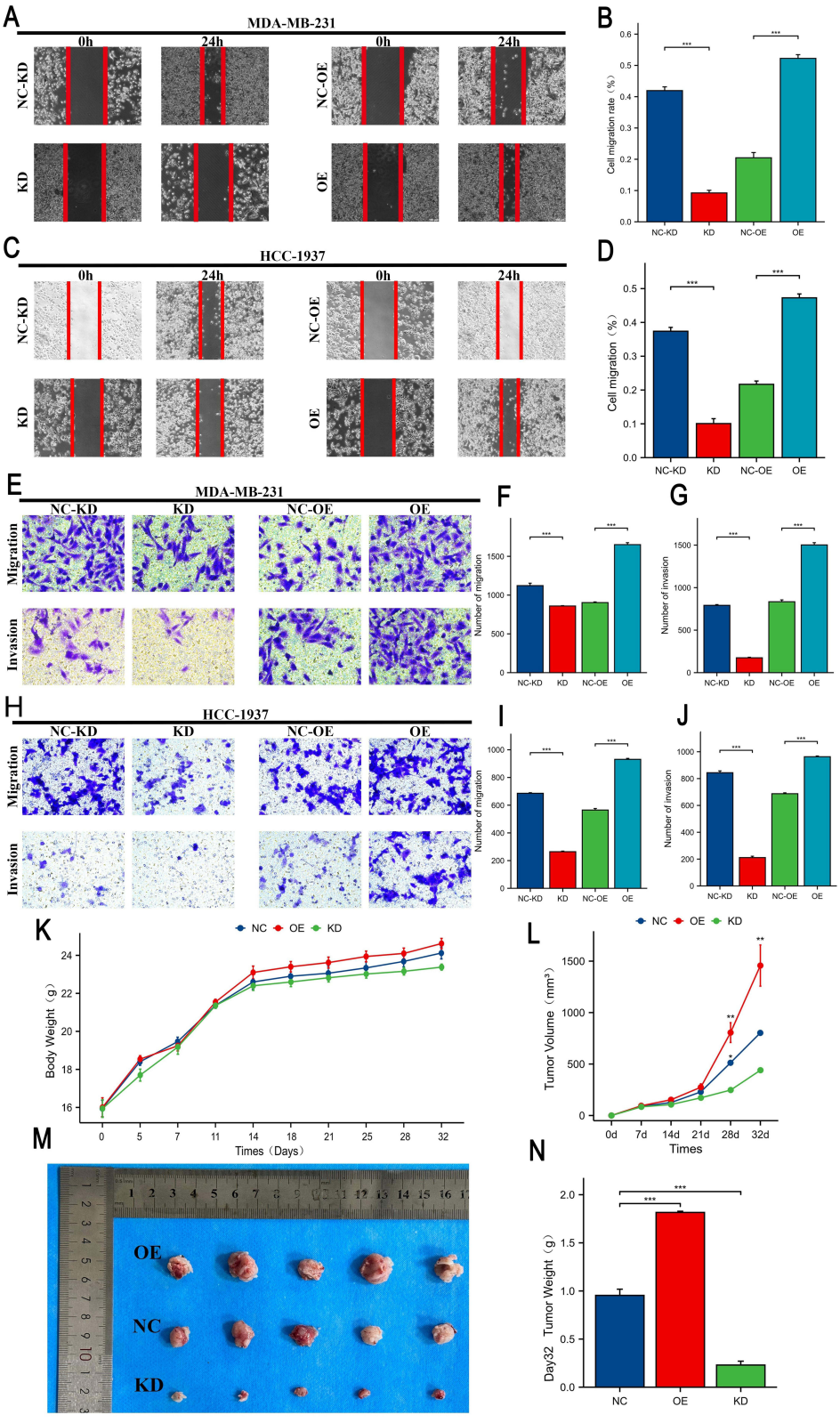

Figure 11 Overexpression of ABHD12 in breast cancer cell lines enhances the invasive and migratory capabilities of breast cancer cells and promotes tumor formation in mice. Scratch assays demonstrate the differential effects of varying ABHD12 expression levels on the migratory capacity of **(A** and **B)** MDA-MB-231 cell line and **(C** and **D)** HCC-1937 cell line. Transwell invasion and migration assays validate the impact of ABHD12 knockdown and overexpression on the invasive and migratory properties of (**E–G**) MDA-MB-231 cell line and (**H–J**) HCC-1937 cell line. (**K–N**) Animal experiments assess the effects of ABHD12 knockdown and overexpression on body weight and tumor mass/volume in NCG mice. *p<0.05, **p<0.01, ***p<0.001.

https://doi.org/10.2147/BCTT.S554836

Epigenetic and epigenomic alterations play a pivotal role in cancer development.[30,31] In this study, methylation analysis revealed inconsistent methylation patterns in the promoter region of ABHD12 across various cancer types. Specifically, reduced methylation levels were observed in certain cancers, such as UCEC and PRAD, whereas significantly elevated methylation was detected in others, including COAD, KIRC, LUSC, SARC, and LIHC. Concurrently, ABHD12 expression showed association with only a subset of m6A regulatory factors, suggesting that its transcriptional regulation may not primarily depend on canonical epigenetic mechanisms, such as promoter methylation. In contrast, genomic variation analysis demonstrated that ABHD12 harbors significant CNVs across multiple tumor types. Moreover, ABHD12 expression levels exhibited a strong correlation with CNV status and were consistently linked to poor prognosis in most cancers. Collectively, these findings indicate that the aberrant expression of ABHD12 in tumors is more likely driven by genomic-level CNVs rather than alterations in promoter methylation. This study is based on batch sequencing data from public databases, lacking functional validation and single-cell resolution. In the future, the regulatory role of CNV on ABHD12 and its biological significance in tumors can be further verified through experimental models. However, it should be noted that this research is based on public batch sequencing data and lacks single-cell resolution and functional validation. In the future, the causal relationship can be further clarified by constructing a CNV editing model.

The metabolic plasticity of macrophages plays a pivotal role in immunopathology and tumor immunotherapy.[32,33] While M1 macrophages primarily exert pro-inflammatory and anti-tumor effects, M2 macrophages tend to suppress inflammation and promote angiogenesis.[34] In particular, M2-polarized tumor-associated macrophages (TAMs) have emerged as critical drivers of tumor progression and metastasis, representing potential therapeutic targets.[35] As a sensor of cellular energy status, AMPK plays a decisive role in macrophage polarization.[36] Existing evidence indicates that ABHD12 co-localizes with M2 macrophages in tumor tissues.[8] Concurrently, the activation of AMPKα1 in the tumor microenvironment has been shown to enhance M2 polarization and facilitate tumor development.[37] Interestingly, our data reveal a significant positive correlation between ABHD12 expression and macrophage infiltration levels in Luminal A BRCA, DLBC, HNSC, KIRC, LUAD, LUSC, MESO, SARC, TGCT, and UVM. Furthermore, KEGG pathway enrichment analysis demonstrates that ABHD12 and its associated proteins are significantly enriched in the AMPK signaling pathway, suggesting that ABHD12 may be involved in regulating this pathway. Based on these findings, we hypothesize that ABHD12 may act as an upstream regulator that induces M2 macrophage polarization via the activation of the AMPK pathway, thereby constructing a microenvironment favorable for tumor progression. Whether and how ABHD12 regulates macrophage polarization via the AMPK pathway remains to be further validated through co-culture experiments and in vivo immune models in future studies.

Immune regulation is pivotal in mediating tumor immune rejection and influencing the onset of disease.[38] The emergence of ICB has brought a significant breakthrough in cancer treatment.[39] Investigations have demonstrated that TMB and MSI can be vital markers for determining ICB efficacy,[40,41] while NEO can serve as a potential target for tumor immunotherapy.[42] This investigation indicated that in COAD, ABHD12 expression was negatively correlated with TMB, MSI and NEO levels, suggesting that COAD patients with high ABHD12 expression may have a poorer response to ICB treatment. Conversely, in LIHC, BLCA and SKCM, ABHD12 expression was positively correlated with TMB and MSI levels; while in LUAD, its expression was positively correlated with MSI and NEO levels. These findings indicate that elevated expression of ABHD12 in these cancers may be indicative of increased tumor immunogenicity, thereby providing more abundant neoantigen targets and enhancing the potential response to ICB. Additionally, based on the TISMO database analysis of mouse tumor models, it was shown that in lung cancer, the response group of anti-CTLA-4 combined with anti-PD-1 ICB treatment had significantly higher ABHD12 expression levels than the baseline group. The results of GOKEGG and GSEA analyses also indicated that ABHD12 expression level might be linked to immune-related functions. In conclusion, our findings suggest that ABHD12 may serve as a candidate prognostic biomarker with potential predictive value for immunotherapy response. However, this study relies on publicly available databases and does not include validation with clinical samples or experimental evidence at the mechanistic level. Future research should include additional functional experiments to clarify the specific role of ABHD12 in the tumor immune microenvironment.

Chemotherapy represents a fundamental approach in the management of cancer, and it is often combined with immunotherapy or radiotherapy to augment the healing effect.[43] Abnormal lipid metabolism is closely related to chemotherapy resistance, and the induced cell membrane remodeling can increase the resistance of tumor cells to chemotherapy drugs.[44] Studies have

shown that cancer cells can inhibit ferroptosis through metabolic reprogramming, thereby promoting chemoresistance.[45] This study indicated that high ABHD12 expression is associated with possible resistance to multiple chemotherapy drugs (such as gemcitabine, doxorubicin, and 5-fluorouracil). Recent research indicates that the overexpression of ABHD12 can inhibit the ferroptosis process in fibrosarcoma,[46] and knocking out ABHD12 can make liver cancer cells more sensitive to ferroptosis.[9] The outcomes indicate that ABHD12 might have a significant role in tumor chemotherapy resistance by regulating lipid metabolism or inhibiting the ferroptosis pathway, and targeting ABHD12 may become a potential strategy to reverse resistance and enhance treatment sensitivity. The findings indicate that ABHD12 could be integral to the development of resistance to chemotherapy in tumors by regulating lipid metabolism or inhibiting the ferroptosis pathway. Targeting ABHD12 may become a potential strategy to reverse resistance and enhance treatment sensitivity. However, the aforementioned conclusions are primarily derived from a limited number of in vitro studies, and lack in-depth support from large-scale clinical cohort verification and in vivo mechanism experiments. Despite these limitations, this study still provides important clues and theoretical foundations for further exploring the function of ABHD12 in mediating tumor resistance and regulating ferroptosis.

In this investigation, we found that in 16 pairs of BRCA clinical samples, ABHD12 expression level was significantly elevated in cancerous tissues compared to the corresponding normal tissues. Further, we constructed ABHD12 knockdown and overexpression models in BRCA cell lines, and found that its overexpression significantly enhanced the proliferation, migration, and invasion abilities of BRCA cells. In vivo experiments also showed that the tumors formed by ABHD12-overexpressing mice were larger, indicating a potential trend toward tumor promotion by ABHD12 in BRCA progression. It should be noted that although this study systematically revealed the oncogenic potential of ABHD12 through pan-cancer integration analysis and preliminary functional experiments, there are still some limitations: Firstly, this study represents a preliminary exploration of ABHD12 in BRCA, and the cohort of 16 paired clinical samples is relatively limited. Therefore, further investigations involving larger clinical cohorts are warranted to validate and extend our current observations. Furthermore, while our data demonstrate the oncogenic function of ABHD12 in specific BRCA cell lines and xenograft mouse models, this effect has not been cross-validated across other cancer types. In cell wound scratch assay, while serum starvation and a 24-h window minimized proliferation, residual division cannot be entirely ruled out. Future investigations using inhibitors like Mitomycin C are needed to rigorously isolate the migratory component. Additionally, our in vivo experiments primarily captured the tumorigenic growth phase, and metastasis or survival endpoints were not evaluated. Future research should therefore focus on conducting long-term observation studies to monitor metastatic dissemination and survival rates. Given that high levels of ABHD12 are found in several tumors and correlate with a poor prognosis, it remains to be determined whether its tumorigenic effect is tissue-specific. Moreover, future studies should employ organoid models, patient-derived xenografts (PDX), and single-cell multi-omics technologies to conduct an in-depth investigation into the role of ABHD12 in modulating tumor cell autonomous behavior and regulating the immune microenvironment.

Conclusion

This research found that ABHD12 is significantly overexpressed in various malignant tumors and is strongly correlated with an unfavorable prognosis, diagnostic potential, and treatment resistance. At the mechanism level, the aberrant expression of ABHD12 is likely influenced by CNVs rather than regulation through promoter methylation; its expression level is specifically associated with the tumor immune microenvironment (especially with macrophage), immunotherapy biomarkers (such as TMB, MSI, NEO), and key immune checkpoints, which suggests that ABHD12 levels are potentially associated with the efficacy of immunotherapy in specific tumors. Integrating immune infiltration and KEGG pathway analyses, we found that ABHD12 may regulate macrophage polarization within the tumor immune microenvironment via the AMPK signaling pathway. Additionally, elevated expression levels of ABHD12 have been linked to resistance against multiple chemotherapeutic agents, and may promote treatment resistance by regulating lipid metabolism or inhibiting the ferroptosis pathway. In BRCA, we found through 16 pairs of clinical samples, in vitro cell models, and in vivo xenograft experiments that ABHD12 exhibits a trend toward promoting the proliferation, migration, invasion, and tumorigenic ability of tumor cells, thereby suggesting its potential tumor-promoting function. In summary, ABHD12 is not only a potential biomarker with pan-cancer diagnostic and prognostic value, but may also become a key molecular node connecting lipid metabolism reprogramming, immune microenvironment regulation, and treatment resistance. Future studies can further explore its biological functions and mechanisms of action, and evaluate its potential intervention value in a wider range of tumor models.

Abbreviations

ACC, Adrenocortical Carcinoma; BLCA, Bladder Urothelial Carcinoma; BRCA, Breast Cancer; CESC, Cervical squamous cell carcinoma and endocervical adenocarcinoma; CHOL, Cholangiocarcinoma; CNV, Copy Number Variants; COAD, Colon adenocarcinoma; DLBC, Lymphoid Neoplasm Diffuse Large B-cell Lymphoma; DSS, Disease-specific Survival; ESCA, Esophageal carcinoma; GBM, Glioblastoma multiforme; HNSC, Head and neck squamous cell carcinoma; IHC, Immunohistochemistry; KICH, Kidney chromophobe cell carcinoma; KIRC, Kidney renal clear cell carcinoma; KIRP, Kidney renal papillary cell carcinoma; LAML, Acute Myeloid Leukemia; LGG, Brain Lower Grade Glioma; LIHC, Liver hepatocellular carcinoma; LUAD, Lung adenocarcinoma; LUSC, Lung squamous cell carcinoma; MSI, Microsatellite Instability; NEO, Neoantigen; OS, Overall Survival; OV, Ovarian serous cystadenocarcinoma; PAAD, Pancreatic adenocarcinoma; PFS, Progression-free Survival; PPI, Protein-protein Interaction; PRAD, Prostate adenocarcinoma; READ, Rectum adenocarcinoma; SKCM, Skin Cutaneous Melanoma; STAD, Stomach adenocarcinoma; TGCT, Testicular Germ Cell Tumors; THYM, Thymoma; TMB, Tumor Mutational Burden; TME, Tumor Microenvironment; UCEC, Uterine corpus endometrial carcinoma; UCS, Uterine Carcinosarcoma; WB, Western blotting.

Data Sharing Statement

The original contributions are part of the article/supplementary material. For more details, please get in touch with the corresponding author, Chenming Guo.

Ethics Statement

The research involving human participants was approved by the Ethics Committee of The First Affiliated Hospital of Xinjiang Medical University (Approval No. 230714-07), and all procedures were carried out in accordance with local regulations and institutional guidelines, and the principles of the Declaration of Helsinki. Written informed consent was obtained from all participants prior to their involvement in the study. This study was supervised and reviewed by the Institutional Animal Care and Use Committee (IACUC) of the First Affiliated Hospital of Xinjiang Medical University. Throughout the research, we strictly adhered to the ethical principles and welfare standards for the use of laboratory animals (Approval No. B202411140401).

Author Contributions

Jiawei Zhao, Yuting Gou, and Yiyang Wang share the first authorship. All authors made a significant contribution to the work reported, whether that is in the conception, study design, execution, acquisition of data, analysis and interpretation, or in all these areas; took part in drafting, revising or critically reviewing the article; gave final approval of the version to be published; have agreed on the journal to which the article has been submitted; and agree to be accountable for all aspects of the work.

Funding

National Natural Science Foundation of China (82560576, 32260186), The State Key Laboratory of Pathogenesis, Prevention, Treatment of Central Asian High Incidence Diseases Fund (SKL-HIDCA-2024-21), Outstanding Youth Science Fund (2024D01E22), Xinjiang Uygur Autonomous Region Youth Science and Technology Top-notch Talent Program (2022TSYCCX0029), National Health Commission of the People's Republic of China (WKZX2023WK0109).

Disclosure

The authors report no conflicts of interest in this work.

References

1. Bray F, Laversanne M, Sung H, et al. Global cancer statistics 2022: GLOBOCAN estimates of incidence and mortality worldwide for 36 cancers in 185 countries. *CA Cancer J Clin*. 2024;74:229–263. doi:10.3322/caac.21834
2. Santos CR, Schulze A. Lipid metabolism in cancer. *FEBS J*. 2012;279:2610–2623. doi:10.1111/j.1742-4658.2012.08644.x
3. Lord CC, Thomas G, Brown JM. Mammalian alpha beta hydrolase domain (ABHD) proteins: lipid metabolizing enzymes at the interface of cell signaling and energy metabolism. *Biochim Biophys Acta*. 2013;1831:792–802. doi:10.1016/j.bbalip.2013.01.002
4. Khandelwal N, Shaikh M, Mhetre A, et al. Fatty acid chain length drives lysophosphatidylserine-dependent immunological outputs. *Cell Chem Biol*. 2021;28:1169–79e6. doi:10.1016/j.chembiol.2021.01.008

5. Liu J, Wang Y, Zhao Y, et al. Comprehensive variant analysis of phospholipase A2 superfamily genes in large Chinese Parkinson' s disease cohorts. *Mech Ageing Dev*. 2024;219:111940. doi:10.1016/j.mad.2024.111940
6. Mao T, Zhang M, Peng Z, et al. Integrative analysis of ferroptosis-related genes reveals that ABHD12 is a novel prognostic biomarker and facilitates hepatocellular carcinoma tumorigenesis. *Discov Oncol*. 2024;15:330. doi:10.1007/s12672-024-01211-w
7. Bian J, Xiong W, Yang Z, et al. Identification and prognostic biomarkers among ZDHHC4/12/18/24, and APT2 in lung adenocarcinoma. *Sci Rep*. 2024;14:522. doi:10.1038/s41598-024-51182-9
8. Wu K, Li Y, Ji Y, et al. Tumor-Derived RAB21+ABHD12+ sEVs drive the premetastatic microenvironment in the lung. *Cancer Immunol Res*. 2024;12:161–179. doi:10.1158/2326-6066.CIR-23-0221
9. Cai M, Luo J, Yang C, et al. ABHD12 contributes to tumorigenesis and sorafenib resistance by preventing ferroptosis in hepatocellular carcinoma. *iScience*. 2023;26:108340. doi:10.1016/j.isci.2023.108340
10. Vivian J, Rao AA, Nothaft FA, et al. Toil enables reproducible, open source, big biomedical data analyses. *Nat Biotechnol*. 2017;35:314–316. doi:10.1038/nbt.3772
11. Chandrashekar DS, Karthikeyan SK, Korla PK, et al. UALCAN: an update to the integrated cancer data analysis platform. *Neoplasia*. 2022;25:18–27. doi:10.1016/j.neo.2022.01.001
12. Gao J, Aksoy BA, Dogrusoz U, et al. Integrative analysis of complex cancer genomics and clinical profiles using the cBioPortal. *Sci Signal*. 2013:6: pl1. doi:10.1126/scisignal.2004088
13. Liu CJ, Hu FF, Xie GY, et al. GSCA: an integrated platform for gene set cancer analysis at genomic, pharmacogenomic and immunogenomic levels. *Brief Bioinform*. 2023:24. doi:10.1093/bib/bbac558
14. Chen D, Xu L, Xing H, et al. Sangerbox 2: enhanced functionalities and update for a comprehensive clinical bioinformatics data analysis platform. *Imeta*. 2024:3e238. doi:10.1002/imt2.238
15. Bindea G, Mlecnik B, Tosolini M, et al. Spatiotemporal dynamics of intratumoral immune cells reveal the immune landscape in human cancer. *Immunity*. 2013;39:782–795. doi:10.1016/j.immuni.2013.10.003
16. Li T, Fu J, Zeng Z, et al. TIMER2.0 for analysis of tumor-infiltrating immune cells. *Nucleic Acids Res*. 2020:48:W509–W14. doi:10.1093/nar/gkaa407
17. Zeng Z, Wong CJ, Yang L, et al. TISMO: syngeneic mouse tumor database to model tumor immunity and immunotherapy response. *Nucleic Acids Res*. 2022;50:D1391–D7. doi:10.1093/nar/gkab804
18. Szklarczyk D, Kirsch R, Koutrouli M, et al. The STRING database in 2023: protein-protein association networks and functional enrichment analyses for any sequenced genome of interest. *Nucleic Acids Res*. 2023:51:D638–D46. doi:10.1093/nar/gkac1000
19. Tang Z, Kang B, Li C, et al. GEPIA2: an enhanced web server for large-scale expression profiling and interactive analysis. *Nucleic Acids Res*. 2019:47:W556–W60. doi:10.1093/nar/gkz430
20. Shannon P, Markiel A, Ozier O, et al. Cytoscape: a software environment for integrated models of biomolecular interaction networks. *Genome Res*. 2003;13:2498–2504. doi:10.1101/gr.1239303
21. Kanehisa M, Furumichi M, Sato Y, et al. KEGG: biological systems database as a model of the real world. *Nucleic Acids Res*. 2025;53:D672–D7. doi:10.1093/nar/gkae909
22. Gou Y, Li Y, Wang Y, et al. Integrated pan-cancer profiling and breast cancer validation identify BEND3 as a potential prognostic and immune biomarker. *Breast Cancer*. 2025;17:1439–1461. doi:10.2147/BCTT.S553681
23. Yuan Q, Zhang H, Zhang N, et al. BPHL promotes TNBC stemness by resolving R-loops via POLR2A lactylation inhibition and BARD1-mediated ubiquitination. *Cancer Lett*. 2026;645:218388. doi:10.1016/j.canlet.2026.218388
24. Feng L, Yuan Q, Yu H, et al. Identification of biomarkers associated with exhausted CD8 + T cells in the tumor microenvironment of intrahepatic cholangiocarcinoma based on Mendelian randomization and bioinformatics analysis. *Discov Oncol*. 2025;16:1092. doi:10.1007/s12672-025-02970-w
25. Nardini M, Dijkstra BW. Alpha/beta hydrolase fold enzymes: the family keeps growing. *Curr Opin Struct Biol*. 1999;9:732–737. doi:10.1016/s0959-440x(99)00037-8
26. Yang S, Li M, Lian G, et al. ABHD8 antagonizes inflammation by facilitating chaperone-mediated autophagy-mediated degradation of NLRP3. *Autophagy*. 2025;21:338–351. doi:10.1080/15548627.2024.2395158
27. Wang S, Xing X, Ma J, et al. Deacylases-structure, function, and relationship to diseases. *FEBS Lett*. 2024;598:959–977. doi:10.1002/1873-3468.14885
28. Cao Y, Qiu T, Kathayat RS, et al. ABHD10 is an S-depalmitoylase affecting redox homeostasis through peroxiredoxin-5. *Nat Chem Biol*. 2019;15:1232–1240. doi:10.1038/s41589-019-0399-y
29. Shi X, Li X, Xu Z, et al. ABHD16A negatively regulates the palmitoylation and antiviral function of IFITM proteins. *mBio*. 2022;13:e0228922. doi:10.1128/mbio.02289-22
30. Shen H, Laird PW. Interplay between the cancer genome and epigenome. *Cell*. 2013;153:38–55. doi:10.1016/j.cell.2013.03.008
31. Kiri S, Ryba T. Cancer, metastasis, and the epigenome. *Mol Cancer*. 2024;23:154. doi:10.1186/s12943-024-02069-w
32. Wang S, Liu R, Yu Q, et al. Metabolic reprogramming of macrophages during infections and cancer. *Cancer Lett*. 2019;452:14–22. doi:10.1016/j.canlet.2019.03.015
33. Wang J, Li Z, Gao L, et al. The regulation effect of AMPK in immune related diseases. *Sci China Life Sci*. 2018;61:523–533. doi:10.1007/s11427-017-9169-6
34. Zhou S, Lan Y, Li Y, et al. Hypoxic tumor-derived exosomes induce M2 macrophage polarization via PKM2/AMPK to promote lung cancer progression. *Cell Transplant*. 2022;31:9636897221106998. doi:10.1177/09636897221106998
35. Xu F, Cui WQ, Wei Y, et al. Astragaloside IV inhibits lung cancer progression and metastasis by modulating macrophage polarization through AMPK signaling. *J Exp Clin Cancer Res*. 2018;37:207. doi:10.1186/s13046-018-0878-0
36. Cui Y, Chen J, Zhang Z, et al. The role of AMPK in macrophage metabolism, function and polarisation. *J Transl Med*. 2023;21:892. doi:10.1186/s12967-023-04772-6
37. Qiu S, Liu T, Piao C, et al. AMPKalpha2 knockout enhances tumour inflammation through exacerbated liver injury and energy deprivation-associated AMPKalpha1 activation. *J Cell Mol Med*. 2019;23:1687–1697. doi:10.1111/jcmm.13978
38. Devaud C, John LB, Westwood JA, et al. Immune modulation of the tumor microenvironment for enhancing cancer immunotherapy. *Oncoimmunology*. 2013;2:e25961. doi:10.4161/onci.25961

39. Wang Y, Wang M, Wu HX, et al. Advancing to the era of cancer immunotherapy. *Cancer Commun*. 2021;41:803–829. doi:10.1002/cac2.12178
40. Baretti M, Le DT. DNA mismatch repair in cancer. *Pharmacol Ther*. 2018;189:45–62. doi:10.1016/j.pharmthera.2018.04.004
41. Xu Y, Fu Y, Zhu B, et al. Predictive biomarkers of immune checkpoint inhibitors-related toxicities. *Front Immunol*. 2020;11:2023. doi:10.3389/fimmu.2020.02023
42. Schumacher TN, Schreiber RD. Neoantigens in cancer immunotherapy. *Science*. 2015;348:69–74. doi:10.1126/science.aaa4971
43. Li Q, Lei X, Zhu J, et al. Radiotherapy/Chemotherapy-Immunotherapy for cancer management: from mechanisms to clinical implications. *Oxid Med Cell Longev*. 2023;2023:7530794. doi:10.1155/2023/7530794
44. Qin J, Ye L, Wen X, et al. Fatty acids in cancer chemoresistance. *Cancer Lett*. 2023;572:216352. doi:10.1016/j.canlet.2023.216352
45. Nie Z, Chen M, Gao Y, et al. Ferroptosis and tumor drug resistance: current status and major challenges. *Front Pharmacol*. 2022;13:879317. doi:10.3389/fphar.2022.879317
46. Kathman SG, Boshart J, Jing H, et al. Blockade of the lysophosphatidylserine lipase ABHD12 potentiates ferroptosis in cancer cells. *ACS Chem Biol*. 2020;15:871–877. doi:10.1021/acschembio.0c00086